

# Tris-Thiourea Tripodal-based Molecules as Chloride transmembrane Transporters: Insights from Molecular Dynamics Simulations

Igor Marques,<sup>a)</sup> Ana R. Colaço,<sup>a)</sup> Paulo J. Costa,<sup>b)</sup> Nathalie Busschaert,<sup>c)</sup> Philip A. Gale,<sup>c)</sup> and Vítor Félix<sup>a)\*</sup>

\* vitor.felix@ua.pt

## *Electronic Supplementary Information*

### **Contents**

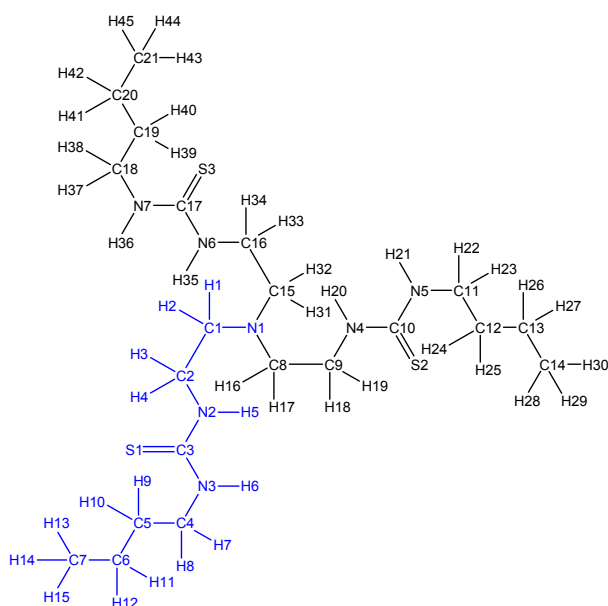
Transporters' 1-6 atom names, atom types and atomic RESP charges.....	5
Conformational analysis on 1-6 chloride complexes .....	11
Analysis of free membrane system A.....	13
Supporting figures for simulations B-G.....	18
Supporting figures for simulation H.....	27
Supporting figures for simulation H' .....	28
Methods of preliminary MD simulation in water solution and supporting figures for simulation E' .....	28
Supporting figures for the evaluation of the impact of 1-6 onto the POPC membrane.....	35
References.....	40
Table S1. Atom types and RESP charges employed for 1.....	5
Table S2. Atom types and RESP charges employed for 2.....	6
Table S3. Atom types and RESP charges employed for 3.....	7
Table S4. Atom types and RESP charges employed for 4.....	8
Table S5. Atom types and RESP charges employed for 5.....	9
Table S6. Atom types and RESP charges employed for 6.....	10
Table S7. Dimensions of N-H...Cl <sup>-</sup> bonds found in the MM energy minimized structures of 1-6⊃Cl <sup>-</sup> .	11
Table S8. N-C-C-N torsion angles (°) in gas phase for 1-6 chloride complexes. ....	11
Table S9. Structural parameters for area per lipid and bilayer thickness of system A, with the corresponding standard deviations, for 100 ns of sampling. Literature values are given for comparison purposes. ....	14
Table S10. Water solution simulated systems at 303 K for 30 ns. ....	29
Scheme S1. Atomic numbering scheme for 1.....	5
Scheme S2. Atomic numbering scheme for 2.....	6
Scheme S3. Atomic numbering scheme for 3.....	7
Scheme S4. Atomic numbering scheme for 4.....	8
Scheme S5. Atomic numbering scheme for 5.....	9
Scheme S6. Atomic numbering scheme for 6.....	10
Figure S1. MM lowest energy structure of 1⊃Cl <sup>-</sup> with N-H...Cl <sup>-</sup> hydrogen bonds shown as red dashed lines. The carbon, nitrogen, sulfur and hydrogen atoms are drawn in light grey, blue, yellow and white, respectively. The chloride anion is represented in green. ....	11

Figure S2. MM lowest energy structure of 2 $\Rightarrow$ Cl <sup>-</sup> with N-H $\cdots$ Cl <sup>-</sup> hydrogen bonds shown as red dashed lines. The carbon, nitrogen, sulfur and hydrogen atoms are drawn in light grey, blue, yellow and white, respectively. The chloride anion is represented in green. ....	11
Figure S3. MM lowest energy structure of 3 $\Rightarrow$ Cl <sup>-</sup> with N-H $\cdots$ Cl <sup>-</sup> hydrogen bonds shown as red dashed lines. The carbon, nitrogen, sulfur, fluorine and hydrogen atoms are drawn in light grey, blue, yellow, cyan and white, respectively. The chloride anion is represented in green.....	12
Figure S4. MM lowest energy structure of 5 $\Rightarrow$ Cl <sup>-</sup> with N-H $\cdots$ Cl <sup>-</sup> hydrogen bonds shown as red dashed lines. The carbon, nitrogen, sulfur, fluorine and hydrogen atoms are drawn in light grey, blue, yellow, cyan and white, respectively. The chloride anion is represented in green.....	12
Figure S5. MM lowest energy structure of 6 $\Rightarrow$ Cl <sup>-</sup> with N-H $\cdots$ Cl <sup>-</sup> hydrogen bonds shown as red dashed lines. The carbon, nitrogen, sulfur, fluorine and hydrogen atoms are drawn in light grey, blue, yellow, cyan and white, respectively. The chloride anion is represented in green.....	12
Figure S6. Evolution of area per lipid ( <i>a</i> ) and bilayer thickness ( <i>b</i> ) in system A through the course of the MD simulation time. The reference values are plotted as green (experimental) and magenta (theoretical) lines, at 303 K <sup>5</sup> . The red and blue lines correspond to each one of the two replicates. ....	13
Figure S7. Electron density profiles of system A, with the full system plotted in black, water in blue, phospholipids in green and phosphorus atoms in orange. The <i>z</i> = 0 Å corresponds to the core of the POPC bilayer. In plot <i>a</i> , the X-ray scattering of the POPC bilayer profile is also shown as a pink line. <sup>5</sup> In plot <i>b</i> , the calculated full system electron density profile for the POPC bilayer on the LIPID11 paper is also shown as a red line. <sup>6</sup> .....	15
Figure S8. Computed  S <sub>CD</sub>   for palmitoyl and oleyl chains for 100 ns of sampling of system A. The  S <sub>CD</sub>   values calculated for the <i>sn</i> -1 chain are shown in red, while the values for the <i>sn</i> -2 chain are shown in green. The error bars associated with these results correspond to the SD. In plot <i>a</i> , the experimental values for the <i>sn</i> -1 chain were taken from refs. 8 (blue □) and 9 (magenta ○), while the values for the the <i>sn</i> -2 chain were taken from refs. 10 (brown ■) and 9 (orange ●). In plot <i>b</i> , the computed  SCD  values from the LIPID11 paper, <sup>6</sup> with the <i>sn</i> -1 chain values presented as blue □, and the <i>sn</i> -2 chain values presented as brown ■ .....	16
Figure S9. Variation in the number of water molecules within the solvation shell defined by a cut-off of 3.5 Å from 1 (simulations B1 and B2), 2 (simulations C1 and C2), 5 (simulations F1 and F2) or 6 (simulations G1 and G2). Data was smoothed using Bézier curves.....	18
Figure S10. Evolution of N $\cdots$ P <sub>int</sub> and C <sub><i>n</i></sub> $\cdots$ P <sub>int</sub> distances for 1, 2, 5 and 6, for 100 ns, in simulations B1, B2, C1, C2, F1, F2, G1 and G2. C <sub>1</sub> , C <sub>2</sub> and C <sub>3</sub> $\cdots$ P <sub>int</sub> are shown in green, dark blue and magenta lines, N $\cdots$ P <sub>int</sub> is shown as a cyan line, while the water-lipid interface is represented as a black line at <i>z</i> = 0 Å. Data was smoothed using Bézier curves.....	19
Figure S11. Average number of hydrogen bonds vs. the relative position of the COM of 1 (simulations B1 and B2), 2 (simulations C1 and C2), 4 (simulations D1 and D2) and 5 (simulations D1 and D2). The following colour scheme was used for the interactions between the receptor and sulfur atoms (brown), chloride ion (green), water molecules (cyan), POPC head groups (orange), ester groups (purple for the <i>sn</i> -1 chains and magenta for the <i>sn</i> -2 chains).....	20
Figure S12. Hydrogen bonds counting for the interactions established by the NH groups of 1 (simulations B1 and B2), 2 (simulations C1 and C2) and 3 (simulations D1 and D2). The following colour scheme was used for the interactions between the receptor and sulfur atoms (brown), chloride ion (green), water molecules (cyan), POPC head groups (orange), ester groups (purple for the <i>sn</i> -1 chains and magenta for the <i>sn</i> -2 chains). ....	21
Figure S13. Hydrogen bonds counting for the interactions established by the NH groups of 4 (simulations E1 and E2), 5 (simulations F1 and F2) and 6 (simulations G1 and G2). The following colour scheme was used for the interactions between the receptor and sulfur atoms (brown), chloride ion (green), water molecules (cyan), POPC head groups (orange), ester groups (purple for the <i>sn</i> -1 chains and magenta for the <i>sn</i> -2 chains). ....	22
Figure S14. Frequency histograms showing the distribution of the three N-C-C-N torsion angles values of 1 and 2 in simulations B1, B2, C1 and C2, before the interaction with the interface ( <i>pre interaction</i> ) and after ( <i>post interaction</i> ).....	23
Figure S15. Frequency histograms showing the distribution of the three N-C-C-N torsion angles values of 5 and 6 in simulations F1, F2, G1 and G2, before the interaction with the interface ( <i>pre interaction</i> ) and after ( <i>post interaction</i> ).....	24
Figure S16. Variations in the three N-C-C-N tripodal torsion angles for 100 ns of MD simulation, extracted every 500 ps, for simulations B1, B2, C1, C2, D1 and D2, containing 1, 2 or 3. ....	25

Figure S17. Variations in the three N-C-C-N tripodal torsion angles for 200ns of MD simulation E or 100 ns of MD simulations F and G, extracted every 500 ps, for simulations E1, E2, F1, F2, G1 and G2, containing 4, 5 or 6. ....	26
Figure S18. Hydrogen bonds counting for the interactions established by the NH groups of 3 (simulations H1 and H2). The following colour scheme was used for the interactions between the receptor and sulfur atoms (brown), chloride ion (green), water molecules (cyan), POPC head groups (orange), ester groups (purple for the <i>sn</i> -1 chains and magenta for the <i>sn</i> -2 chains).....	27
Figure S19. Variations in the three N-C-C-N tripodal torsion angles for 150 ns of MD simulation, extracted every 500 ps, for simulations H1 and H2, containing 3.....	27
Figure S20. Evolution of COM $\cdots$ P $_{int}$ distances for 3, Cl $\cdots$ P $_{int}$ and N $_{C'}\cdots$ P $_{int}$ in simulations H'1 and H'2, during the 150 ns of simulation time. COM $\cdots$ P $_{int}$ is shown in orange, Cl $\cdots$ P $_{int}$ is shown in red, and N $_{C'}\cdots$ P $_{int}$ is shown in blue, while the water-lipid interface is represented as a black line at z = 0 Å. ....	28
Figure S21. Evolution of the 1-6 $_{COM}\cdots$ Cl $^{-}$ distances (cyan line) and variations in the three N-C-C-N tripodal torsion angles (blue, green and magenta lines), in simulations a-f for 30 ns. All parameters were extracted every 50 ps. ....	30
Figure S22. Hydrogen bonds counting for the interactions established by the NH groups of 1-6 in simulations a-f. The following colour scheme was used for the interactions between the receptor and sulfur atoms (brown), chloride ion (green), and water molecules (cyan).....	31
Figure S23. Evolution of the 1-6 $_{COM}\cdots$ Cl $^{-}$ distances (cyan line) and variations in the three N-C-C-N tripodal torsion angles (blue, green and magenta lines), in simulations g-l for 30 ns. All parameters were extracted every 50 ps. ....	32
Figure S+24. Hydrogen bonds counting for the interactions established by the NH groups of 1-6 in simulations g-l. The following colour scheme was used for the interactions between the receptor and sulfur atoms (brown), chloride ion (green), and water molecules (cyan).....	33
Figure S25. Variations in the three N-C-C-N tripodal torsion angles for 150 ns of MD simulations E'1 and E'2, extracted every 500 ps, for simulations E'1 and E22, containing 4 $\supset$ Cl $^{-}$ .....	34
Figure S26. Average number of hydrogen bonds vs. the relative position of the COM of 4 (simulations E'1 and E'2). The following colour scheme was used for the interactions between the receptor and sulfur atoms (brown), chloride ion (green), water molecules (cyan), POPC head groups (orange), ester groups (purple for the <i>sn</i> -1 chains and magenta for the <i>sn</i> -2 chains).....	34
Figure S27. Electron density profiles of simulations B1, B2, C1, C2, D1 and D2 with the full system plotted in black, water in blue, phospholipids in green, phosphorus atoms in orange and the corresponding transporter profile in red (scaled 5 times). The z = 0 Å corresponds to the core of the POPC bilayer. The POPC bilayer profile of system A is also shown as a pink line. ....	35
Figure S28. Electron density profiles of simulations E1, E2, F1, F2, G1 and G2 with the full system plotted in black, water in blue, phospholipids in green, phosphorus atoms in orange and the corresponding transporter profile in red (scaled 5 times). The z = 0 Å corresponds to the core of the POPC bilayer. The POPC bilayer profile of system A is also shown as a pink line. ....	36
Figure S29. Computed  S $_{CD}$   for palmitoyl and oleyl chains for 25 ns of sampling of simulations B1, B2, C1, C2, D1 and D2. The  S $_{CD}$   values calculated for the <i>sn</i> -1 chain are shown in red, while the values for the <i>sn</i> -2 chain are shown in green. The error bars associated with these results correspond to the SD. The computed  S $_{CD}$   values from system A are presented as blue $\square$ ( <i>sn</i> -1 chain), and brown $\blacksquare$ ( <i>sn</i> -2 chain). ....	37
Figure S30. Computed  S $_{CD}$   for palmitoyl and oleyl chains for 40 ns of sampling of simulations E1, E2, and 25 ns of sampling in simulations F1, F2, G1 and G2. The  S $_{CD}$   values calculated for the <i>sn</i> -1 chain are shown in red, while the values for the <i>sn</i> -2 chain are shown in green. The error bars associated with these results correspond to the SD. The computed  S $_{CD}$   values from system A are presented as blue $\square$ ( <i>sn</i> -1 chain), and brown $\blacksquare$ ( <i>sn</i> -2 chain).....	38
Figure S31. Electron density profiles of simulations H1 and H2 with the full system plotted in black, water in blue, phospholipids in green, phosphorus atoms in orange and the 3's profile in red (scaled 5 times). The z = 0 Å corresponds to the core of the POPC bilayer. The POPC bilayer profile reported on the LIPID11 paper is also shown as a pink line.....	39
Figure S32. Computed  S $_{CD}$   for palmitoyl and oleyl chains for 50 ns of sampling of simulations H1 and H2. The  S $_{CD}$   values calculated for the <i>sn</i> -1 chain are shown in red, while the values for the <i>sn</i> -2 chain are shown in green. The error bars associated with these results correspond to the	

SD. The computed  $|S_{CD}|$  values from the LIPID11 paper are presented as blue  $\square$  (*sn*-1 chain), and brown  $\blacksquare$  (*sn*-2 chain) .....39

## Transporters' 1-6 atom names, atom types and atomic RESP charges



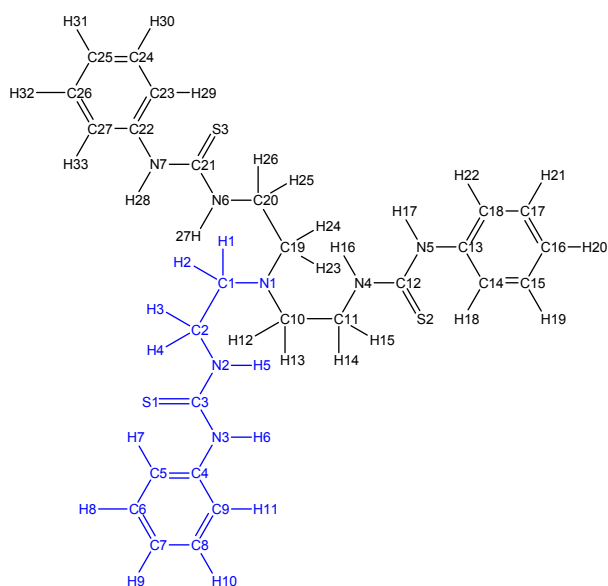
**Scheme S1.** Atomic numbering scheme for **1**.

**Table S1.** Atom types and RESP charges employed for **1**.

Atom name <sup>a)</sup>			Atom type <sup>b)</sup>	Charge
	<b>N1</b>		n3	-0.385382
C1	C8	C15	c3	0.023542
H1	H16	H31	h1	0.044903
H2	H17	H32	h1	0.044903
C2	C9	C16	c3	0.132033
H3	H18	H33	h1	0.027340
H4	H19	H34	h1	0.027340
N2	N4	N6	n	-0.277009
H5	H20	H35	hn	0.262171
C3	C10	C17	c	0.163824
S1	S2	S3	s	-0.469195
N3	N5	N7	n	-0.256867
H6	H21	H36	hn	0.224197
C4	C11	C18	c3	0.109908
H7	H22	H37	h1	0.013275
H8	H23	H38	h1	0.013275
C5	C12	C19	c3	0.021199
H9	H24	H39	hc	0.000955
H10	H25	H40	hc	0.000955
C6	C13	C20	c3	0.105125
H11	H26	H41	hc	-0.016784
H12	H27	H42	hc	-0.016784
C7	C14	C21	c3	-0.165864
H13	H28	H43	hc	0.038673
H14	H29	H44	hc	0.038673
H15	H30	H45	hc	0.038673

<sup>a)</sup> corresponding to the atom numbers shown in Scheme S1.

<sup>b)</sup> according to GAFF.



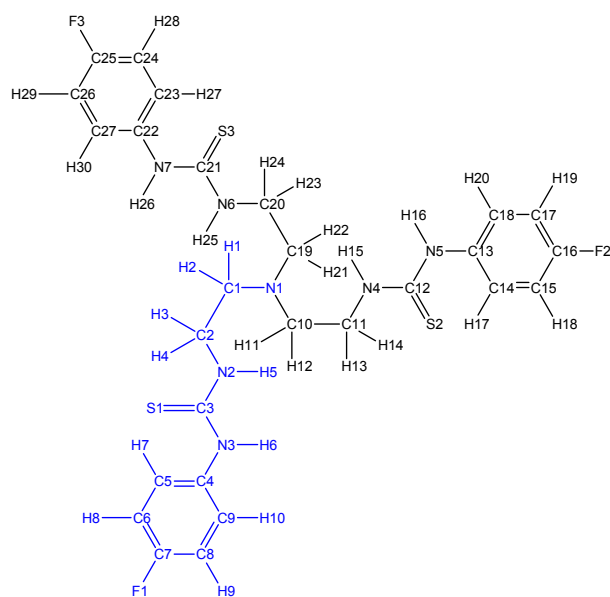
**Scheme S2.** Atomic numbering scheme for **2**.

**Table S2.** Atom types and RESP charges employed for **2**.

Atom name <sup>a)</sup>		Atom type <sup>b)</sup>	Charge
<b>N1</b>		n3	-0.332331
C1	C10 C19	c3	-0.006217
H1	H12 H23	h1	0.062082
H2	H13 H24	h1	0.062082
C2	C11 C20	c3	0.004499
H3	H14 H25	h1	0.064351
H4	H15 H26	h1	0.064351
N2	N4 N6	n	-0.316948
H5	H16 H27	hn	0.324643
C3	C12 C21	c	0.258882
S1	S2 S3	s	-0.475641
N3	N5 N7	n	-0.419973
H6	H17 H28	hn	0.265477
C4	C13 C22	ca	0.414192
C5	C14 C23	ca	-0.317824
H7	H18 H29	ha	0.186913
C6	C15 C24	ca	-0.093026
H8	H19 H30	ha	0.141836
C7	C16 C25	ca	-0.173755
H9	H20 H31	ha	0.146955
C8	C17 C26	ca	-0.093026
H10	H21 H32	ha	0.141836
C9	C18 C27	ca	-0.317824
H11	H22 H33	ha	0.186913

<sup>a)</sup> corresponding to the atom numbers shown in Scheme S2.

<sup>b)</sup> according to GAFF.



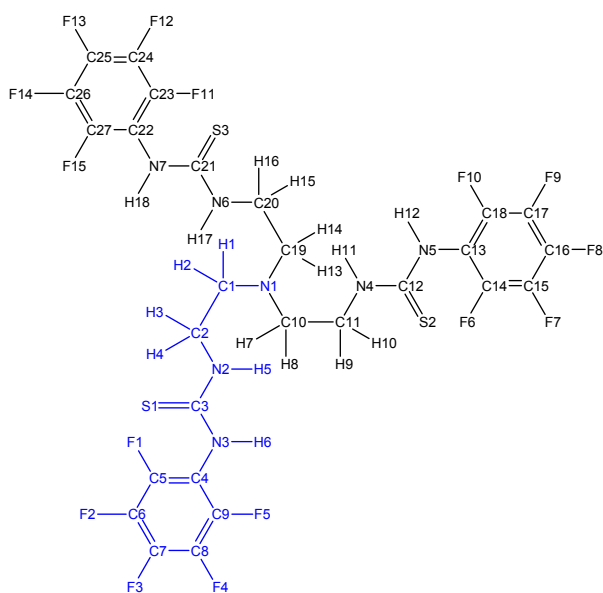
**Scheme S3.** Atomic numbering scheme for **3**.

**Table S3.** Atom types and RESP charges employed for **3**.

Atom name <sup>a)</sup>			Atom type <sup>b)</sup>	Charge
<b>N1</b>			n3	-0.403017
C1	C10	C19	c3	0.001555
H1	H11	H21	h1	0.070346
H2	H12	H22	h1	0.070346
C2	C11	C20	c3	0.014754
H3	H13	H23	h1	0.062365
H4	H14	H24	h1	0.062365
N2	N4	N6	n	-0.337737
H5	H15	H27	hn	0.330814
C3	C12	C25	c	0.268734
S1	S2	S3	s	-0.470045
N3	N5	N7	n	-0.418214
H6	H16	H26	hn	0.263721
C4	C13	C22	ca	0.332907
C5	C14	C23	ca	-0.257391
H7	H17	H27	ha	0.198383
C6	C15	C24	ca	-0.272271
H8	H18	H28	ha	0.190958
C7	C16	C25	ca	0.377233
F1	F2	F3	f	-0.214163
C8	C17	C26	ca	-0.272271
H9	H19	H29	ha	0.190958
C9	C18	C27	ca	-0.257391
H10	H20	H30	ha	0.198383

<sup>a)</sup> corresponding to the atom numbers shown in Scheme S3.

<sup>b)</sup> according to GAFF.



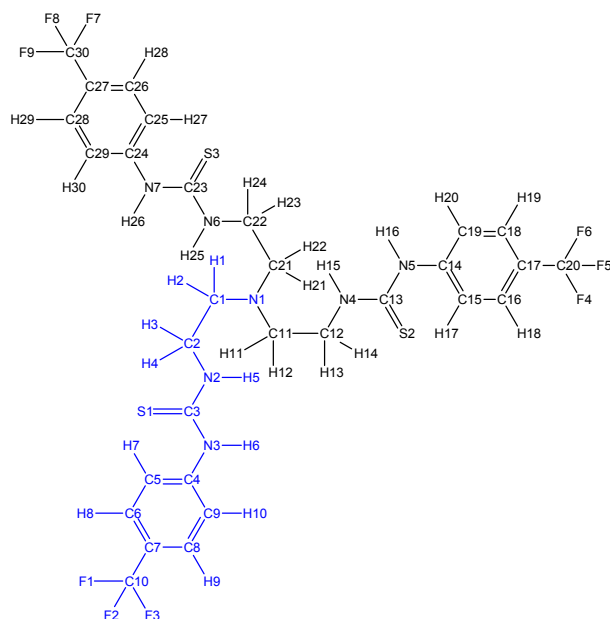
**Scheme S4.** Atomic numbering scheme for **4**.

**Table S4.** Atom types and RESP charges employed for **4**.

Atom name <sup>a)</sup>		Atom type <sup>b)</sup>	Charge
<b>N1</b>		n3	-0.541210
C1	C10 C19	c3	0.041910
H1	H7 H13	h1	0.069046
H2	H8 H14	h1	0.069046
C2	C11 C20	c3	0.015319
H3	H9 H15	h1	0.056645
H4	H10 H16	h1	0.056645
N2	N4 N6	n	-0.217809
H5	H11 H77	hn	0.301320
C3	C12 C21	c	0.192478
S1	S2 S3	s	-0.444777
N3	N5 N7	n	-0.298918
H6	H12 H18	hn	0.298510
C4	C13 C22	ca	-0.045754
C5	C14 C23	ca	0.143247
F1	F6 F11	f	-0.107848
C6	C15 C24	ca	0.127624
F2	F7 F12	f	-0.129391
C7	C16 C25	ca	0.132847
F3	F8 F13	f	-0.113370
C8	C17 C26	ca	0.127624
F4	F9 F14	f	-0.129391
C9	C18 C27	ca	0.143247
F5	F10 F15	f	-0.107848

<sup>a)</sup> corresponding to the atom numbers shown in Scheme S4.

<sup>b)</sup> according to GAFF.



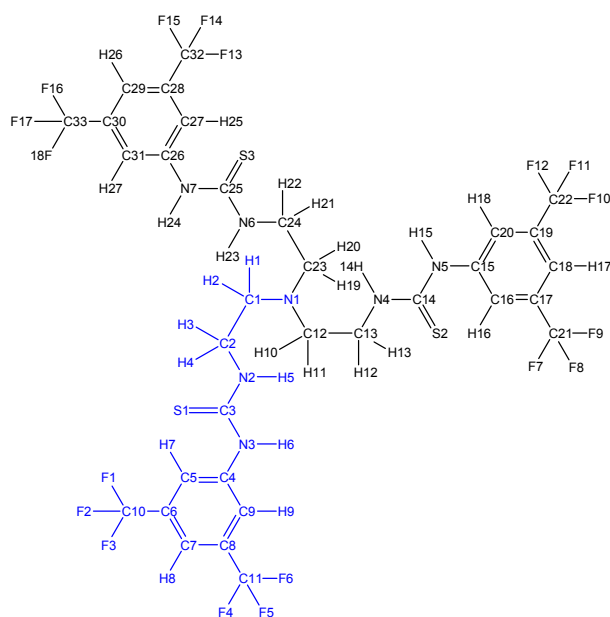
**Scheme S5.** Atomic numbering scheme for **5**.

**Table S5.** Atom types and RESP charges employed for **5**.

Atom name <sup>a)</sup>			Atom type <sup>b)</sup>	Charge
<b>N1</b>			n3	-0.433554
C1	C11	C21	c3	-0.025637
H1	H11	H21	h1	0.080941
H2	H12	H22	h1	0.080941
C2	C12	C22	c3	0.019834
H3	H13	H23	h1	0.062533
H4	H14	H24	h1	0.062533
N2	N4	N6	n	-0.255044
H5	H15	H25	hn	0.295386
C3	C13	C23	c	0.201141
S1	S2	S3	s	-0.452845
N3	N5	N7	n	-0.324809
H6	H16	H26	hn	0.248004
C4	C14	C24	ca	0.335262
C5	C15	C25	ca	-0.273994
H7	H17	H27	ha	0.181205
C6	C16	C26	ca	-0.119715
H8	H18	H28	ha	0.161972
C7	C17	C27	ca	-0.084791
C8	C18	C28	ca	-0.119715
H9	H19	H29	ha	0.161972
C9	C19	C29	ca	-0.273994
H10	H20	H30	ha	0.181205
C10	C20	C30	c3	0.661494
F1	F4	F7	f	-0.219787
F2	F5	F8	f	-0.219787
F3	F6	F9	f	-0.219787

<sup>a)</sup> corresponding to the atom numbers shown in in Scheme S5.

<sup>b)</sup> according to GAFF.



**Scheme S6.** Atomic numbering scheme for **6**.

**Table S6.** Atom types and RESP charges employed for **6**.

Atom name <sup>a)</sup>			Atom type <sup>b)</sup>	Charge
	<b>N1</b>		n3	-0.445817
C1	C12	C23	c3	0.021763
H1	H10	H19	h1	0.061894
H2	H11	H20	h1	0.061894
C2	C13	C24	c3	0.038004
H3	H12	H21	h1	0.063756
H4	H13	H22	h1	0.063756
N2	N4	N6	n	-0.287859
H5	H14	H23	hn	0.267573
C3	C14	C25	c	0.240548
S1	S2	S3	s	-0.441112
N3	N5	N7	n	-0.353971
H6	H15	H24	hn	0.294943
C4	C15	C26	ca	0.268802
C5	C16	C27	ca	-0.249842
H7	H16	H25	ha	0.183127
C6	C17	C28	ca	-0.024046
C7	C18	C29	ca	-0.190350
H8	H17	H26	ha	0.178116
C8	C19	C30	ca	-0.024046
C9	C20	C31	ca	-0.249842
H9	H18	H27	ha	0.183127
C10	C21	C32	c3	0.658502
F1	F7	F13	f	-0.212439
F2	F8	F14	f	-0.212439
F3	F9	F15	f	-0.212439
C11	C22	C33	c3	0.658502
F4	F10	F16	f	-0.212439
F5	F11	F17	f	-0.212439
F6	F12	F18	f	-0.212439

<sup>a)</sup> corresponding to the atom numbers shown in Scheme S6.

<sup>b)</sup> according to GAFF.

## Conformational analysis on 1-6 chloride complexes

**Table S7.** Dimensions of N-H...Cl<sup>-</sup> bonds found in the MM energy minimized structures of **1-6**⊃Cl<sup>-</sup>

Complex	Distance N...Cl <sup>-</sup> (Å)		Angle N-H...Cl <sup>-</sup> (°)	
	Min	Max	Min	Max
<b>1</b> ⊃Cl <sup>-</sup>	3.315	3.519	155.5	166.8
<b>2</b> ⊃Cl <sup>-</sup>	3.341	3.343	160.9	162.6
<b>3</b> ⊃Cl <sup>-</sup>	3.274	3.794	150.4	172.5
<b>4</b> ⊃Cl <sup>-</sup>	3.304	3.321	159.1	160.2
<b>5</b> ⊃Cl <sup>-</sup>	3.262	3.816	149.5	170.7
<b>6</b> ⊃Cl <sup>-</sup>	3.210	3.811	146.3	170.8

**Table S8.** N-C-C-N torsion angles (°) in gas phase for **1-6** chloride complexes.

Chains	Transporter					
	<b>1</b>	<b>2</b>	<b>3</b>	<b>4</b>	<b>5</b>	<b>6</b>
<i>1</i>	52.9	52.8	-50.0	-50.3	50.2	45.3
<i>2</i>	64.7	52.8	-59.5	-50.2	59.0	59.0
<i>3</i>	47.8	52.8	-45.2	-50.3	45.7	49.6

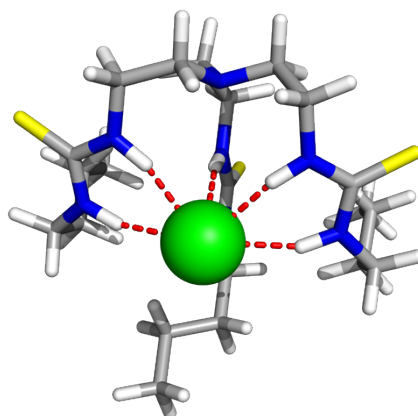


**Figure S1.** MM lowest energy structure of **1**⊃Cl<sup>-</sup> with N-H...Cl<sup>-</sup> hydrogen bonds shown as red dashed lines. The carbon, nitrogen, sulfur and hydrogen atoms are drawn in light grey, blue, yellow and white, respectively. The chloride anion is represented in green.

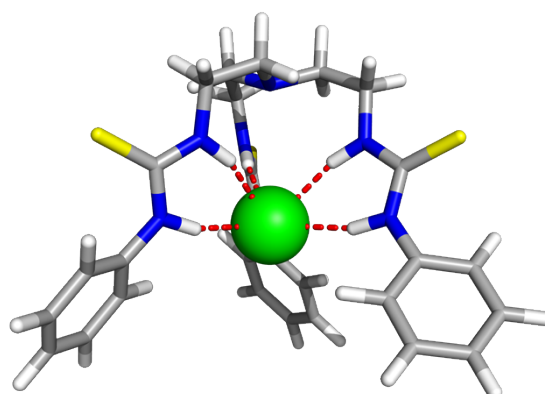


**Figure S2.** MM lowest energy structure of **2**⊃Cl<sup>-</sup> with N-H...Cl<sup>-</sup> hydrogen bonds shown as red dashed lines. The carbon, nitrogen, sulfur and hydrogen atoms are drawn in light grey, blue, yellow and white, respectively. The chloride anion is represented in green.

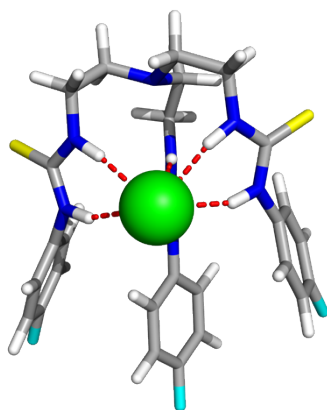


**Figure S3.** MM lowest energy structure of  $3>Cl^-$  with N-H...Cl<sup>-</sup> hydrogen bonds shown as red dashed lines. The carbon, nitrogen, sulfur, fluorine and hydrogen atoms are drawn in light grey, blue, yellow, cyan and white, respectively. The chloride anion is represented in green.

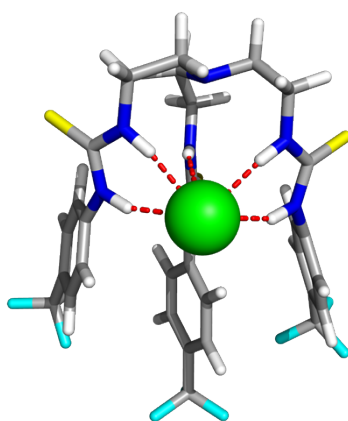


**Figure S4.** MM lowest energy structure of  $5>Cl^-$  with N-H...Cl<sup>-</sup> hydrogen bonds shown as red dashed lines. The carbon, nitrogen, sulfur, fluorine and hydrogen atoms are drawn in light grey, blue, yellow, cyan and white, respectively. The chloride anion is represented in green.

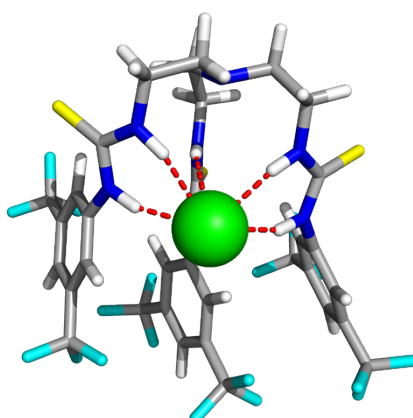


**Figure S5.** MM lowest energy structure of  $6>Cl^-$  with N-H...Cl<sup>-</sup> hydrogen bonds shown as red dashed lines. The carbon, nitrogen, sulfur, fluorine and hydrogen atoms are drawn in light grey, blue, yellow, cyan and white, respectively. The chloride anion is represented in green.

## Analysis of free membrane system A

The equilibration period of system A was established by monitoring the variation of the area per lipid and the related bilayer thickness throughout the course of the MD simulations. The first structural parameter was measured dividing the area of the  $x$ - $y$  section of the system by the number of lipid molecules in each monolayer. In this work, the membrane bilayer thickness was assessed by two different methods: *a*) computing the average distance between the phosphorus atoms of each monolayer along the  $z$  coordinate (see Figure 1); and *b*) measuring the distance between the peaks assigned to the phosphate head groups in the electron density profiles (see below), commonly called the  $D_{\text{HH}}$  distance.<sup>1-4</sup> The evolution of the area per lipid and the bilayer thickness, given by the first method, along the 100 ns of MD simulation are shown in Figure S6 for the two replicates of system A. For the first replicate of this system, the area per lipid and bilayer thickness stabilize after the first 60 ns of simulation time, while for the second replicate these parameters stabilize after 40 ns of simulation. Therefore, those initial long periods were considered equilibration period and were discarded from the subsequent data analysis. The average values of both structural parameters calculated concatenating the last 40 ns of replicate 1 and the last 60 ns of replicate 2, corresponding to a total of 100 ns of sampling from these MD simulations, are gathered in Table S9 for system A.

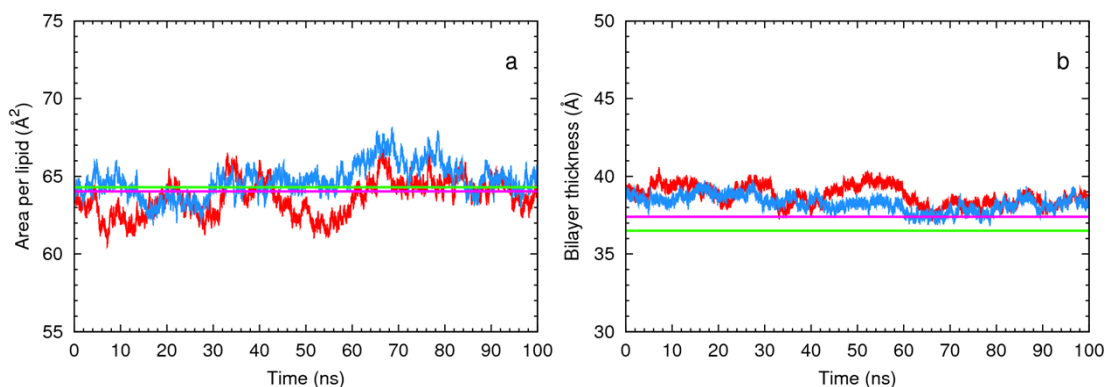


**Figure S6.** Evolution of area per lipid (*a*) and bilayer thickness (*b*) in system A through the course of the MD simulation time. The reference values are plotted as green (experimental) and magenta (theoretical) lines, at 303 K<sup>5</sup>. The red and blue lines correspond to each one of the two replicates.

**Table S9.** Structural parameters for area per lipid and bilayer thickness of system A, with the corresponding standard deviations, for 100 ns of sampling. Literature values are given for comparison purposes.

System	Apl ( $\text{\AA}^2$ )	Bt <sub>1</sub> ( $\text{\AA}$ )	Bt <sub>2</sub> ( $\text{\AA}$ )
A	$64.86 \pm 0.95$	$38.13 \pm 0.42$	36.8
<i>Literature</i>			
X-ray scattering	64.3 <sup>a)</sup>		36.5 <sup>a)</sup>
Computed	$64.03 \pm 1.16$ <sup>b)</sup>		37.4 <sup>b)</sup>

Apl – Area per lipid; Bt<sub>1</sub> – Bilayer thickness measured between phosphorus atoms (method *a*); Bt<sub>2</sub> – Bilayer thickness from the electron density profiles (method *b*); <sup>a)</sup> ref. 5, at 303 K; <sup>b)</sup> ref. 6

As mentioned elsewhere in the main text, these values were obtained with a surface tension of 17 dyn/cm, an optimal value previously reported by Skjevik *et al.*<sup>6</sup> to simulate a POPC bilayer with the LIPID11 force field.

It is noteworthy that the average area computed for system A,  $64.86 \pm 0.95 \text{\AA}^2$ , is in close agreement with the experimental value of  $64.3 \text{\AA}^2$  determined by X-ray scattering at 303 K.<sup>5</sup> Similar conclusions can be extracted with the analysis of the average bilayer thicknesses when assessed by method *a*), as the yielded value ( $38.13 \pm 0.42 \text{\AA}$ ) is close to the  $D_{\text{HH}}$  experimental value,  $36.5 \text{\AA}$  (5% deviation) obtained by X-ray scattering at 303 K,<sup>5</sup> since the  $D_{\text{HH}}$  value depends on more than just the phosphorus atoms in the lipid head groups, as demonstrated below.

The electron density profiles of the over-hydrated POPC bilayer were also evaluated, with recourse to a *ptraj* modification by Hannes Loeffler,<sup>7</sup> concatenating the simulation data from the last 40 ns of replicate 1 and the last 60 ns of replicate 2, thus yielding 100 ns of sampling. This parameter was computed dividing the *z* dimension of the system into slices of  $0.1 \text{\AA}$  and calculating the number of atoms per slice, according to each atom's partial electronic charge. The normalization of the profile was dependent on the division by *x-y* plane average area for the sampling time (average area per lipid of the sampling period times the number of lipids:  $\langle \text{Apl} \rangle \times 64$ ). The electron density profile of system A is plotted in Figure S7 with the individual density profiles for the water slabs, phospholipid bilayer and phosphate head groups represented by the phosphorus atoms. For comparison purposes, the experimental density profile for POPC obtained at 303 K by X-Ray diffraction scattering is also included.<sup>5</sup> The shape of each profile is consistent with the structure of the POPC membrane model along the *z* axis.

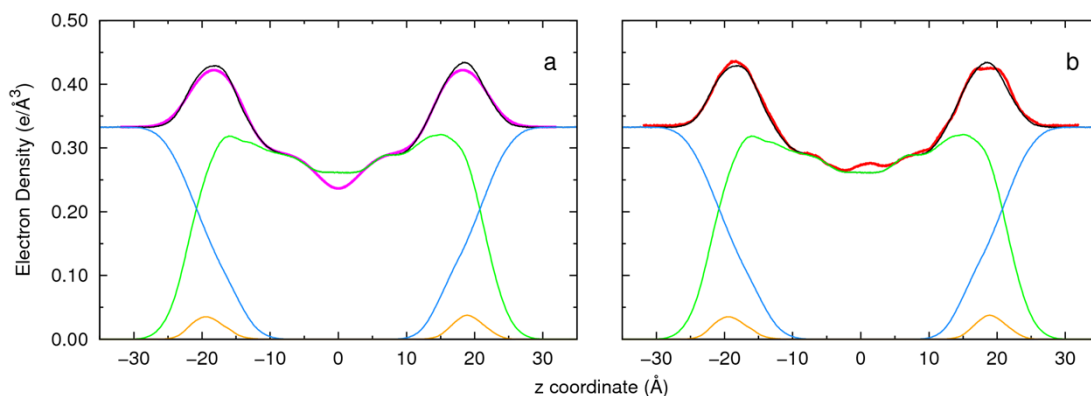


**Figure S7.** Electron density profiles of system A, with the full system plotted in black, water in blue, phospholipids in green and phosphorus atoms in orange. The  $z = 0 \text{ \AA}$  corresponds to the core of the POPC bilayer. In plot *a*, the X-ray scattering of the POPC bilayer profile is also shown as a pink line.<sup>5</sup> In plot *b*, the calculated full system electron density profile for the POPC bilayer on the LIPID11 paper is also shown as a red line.<sup>6</sup>

In fact, the electron density profile (black line) for system A has a symmetric shape around the center of the POPC bilayer with two prominent peaks (distance between peaks:  $36.8 \text{ \AA}$ , consistent with the  $D_{\text{HH}} 36.5 \text{ \AA}$  bilayer thickness obtained by experimental X-ray scattering at  $303 \text{ K}$ <sup>5</sup> and close to the  $37.4 \text{ \AA}$  obtained by Skjevik *et al.*<sup>6</sup>), which are mainly determined by the phosphate groups and to a lesser extent by the choline moieties from the lipids and water molecules between them, as evident when this profile is compared with individual profiles of water slabs (blue line) and phospholipids (green line) and phosphorus atoms (orange line). In these circumstances, using the distance between these latter peaks, bilayer thickness was estimated at *ca.*  $38.3 \text{ \AA}$  (method *b*), which is close to the value calculated using the distance between the opposite bilayer phosphorus heads throughout the course of the MD simulation (method *a*). Also, the small decrease of electron densities at  $z = 0 \text{ \AA}$  (the core of the bilayer) is indicative of potential intercalation between the phospholipid tails of each leaflet. This feature is also observed in the system profile reported by Skjevik *et al.*<sup>6</sup> The overall alignment of the black and magenta lines in *a* shows a good fitting between the theoretical and experimental density profiles, while the alignment between the black and red lines in *b* also indicates a good fitting between the two theoretical profiles.

The ordering of the hydrophobic chains of the POPC lipid molecules, consisting on the relative orientation of the C-H bonds to the bilayer normal, was computationally estimated and compared with the experimental available deuterium order parameters,  $|S_{\text{CD}}|$ ,<sup>8-10</sup> as well as with the values obtained by Skjevik *et al.*<sup>6</sup> The theoretical  $|S_{\text{CD}}|$  values were also calculated with the *ptraj* modification by Hannes Loeffler,<sup>7</sup> using concatenated data from the last 60 ns of each replicate through the equation:

$$|S_{\text{CD}}| = \frac{1}{2}((3\cos^2\theta_i - 1))$$

Where  $\theta_i$  is the angle between the bilayer normal and the  $C_i$ -H bond. The identification of lipid chains and index  $i$  of the carbons in these chains are depicted in Figure S8 (top).

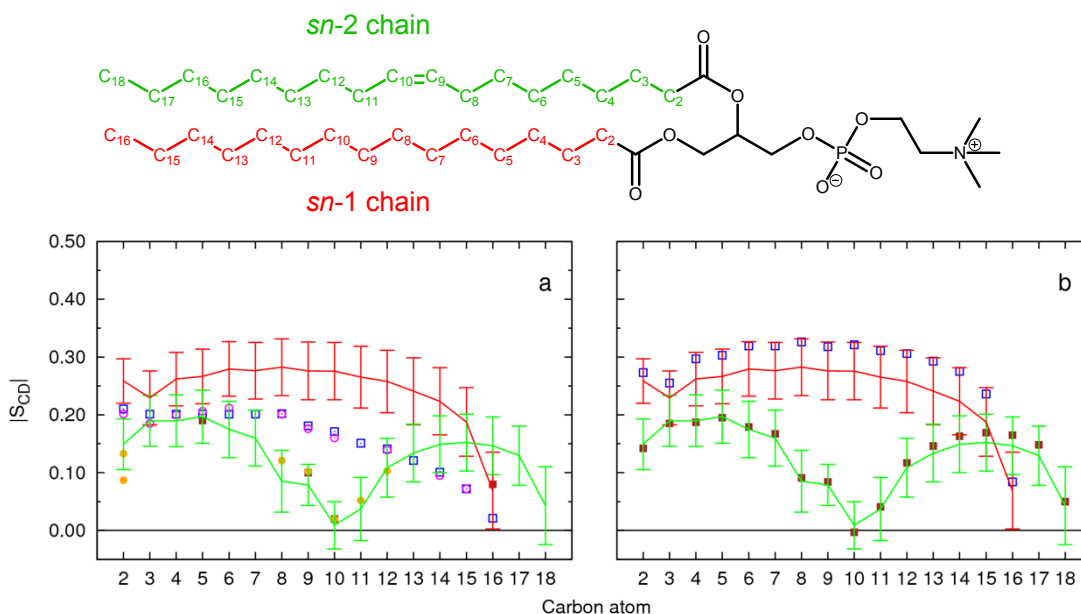


**Figure S8.** Computed  $|S_{CD}|$  for palmitoyl and oleyl chains for 100 ns of sampling of system A. The  $|S_{CD}|$  values calculated for the *sn*-1 chain are shown in red, while the values for the *sn*-2 chain are shown in green. The error bars associated with these results correspond to the SD. In plot *a*, the experimental values for the *sn*-1 chain were taken from refs. 8 (blue  $\square$ ) and 9 (magenta  $\circ$ ), while the values for the the *sn*-2 chain were taken from refs. 10 (brown  $\blacksquare$ ) and 9 (orange  $\bullet$ ). In plot *b*, the computed  $|S_{CD}|$  values from the LIPID11 paper,<sup>6</sup> with the *sn*-1 chain values presented as blue  $\square$ , and the *sn*-2 chain values presented as brown  $\blacksquare$ .

The computed  $|S_{CD}|$  parameters are plotted versus carbon index in Figure S8 for system A, where the values for the *sn*-1 saturated and the *sn*-2 unsaturated chains are shown as red and green lines, respectively, along with the experimental values represented as points.<sup>8-10</sup> Regarding the experimental data, both chains display higher theoretical order parameters for the C-H bonds near the phospholipid heads. Furthermore, as would be expected, the order parameters for the *sn*-2 chain present the lowest values at the double bond between the carbon atoms  $C_9$  and  $C_{10}$  (see Figure 5).<sup>9,10</sup>

The computed *sn*-1 parameters for system A are systematically overestimated when compared with experimental ones, as expected for the LIPID11 force field. Nonetheless, the inflexion of the calculated  $|S_{CD}|$  values for the first two carbons on this chain matches the behavior presented in the experimental data.

In contrast with *sn*-1, the two sets of experimental data available for the *sn*-2 order parameters are composed of few points, with different values for the same carbon index (see Figure S8), thus complicating the comparison with the computed values. Nevertheless, for system A, the theoretical values are close to the

experimental ones. This is particularly evident for the C-H bonds involving the double bonded C<sub>9</sub> and C<sub>10</sub> carbon atoms. The computed order parameters for both phospholipid aliphatic chains follow the theoretical pattern previously reported by Skjevik *et al.*<sup>6</sup>

With the data above, it is demonstrated that the over-hydration of the 128 POPC bilayer has a negligible effect on the structural parameters evaluated, which are mostly accurately reproduced as in the fully hydrated POPC bilayer model.<sup>6</sup> The small differences are ascribed to the different sampling and the effect of the surface tension on a larger periodic cell. Subsequently, this membrane model was used to investigate the passive diffusion of **1-6** chloride complexes across the POPC bilayer, being used as the reference for the evaluation of the structural parameters.

## Supporting figures for simulations B-G

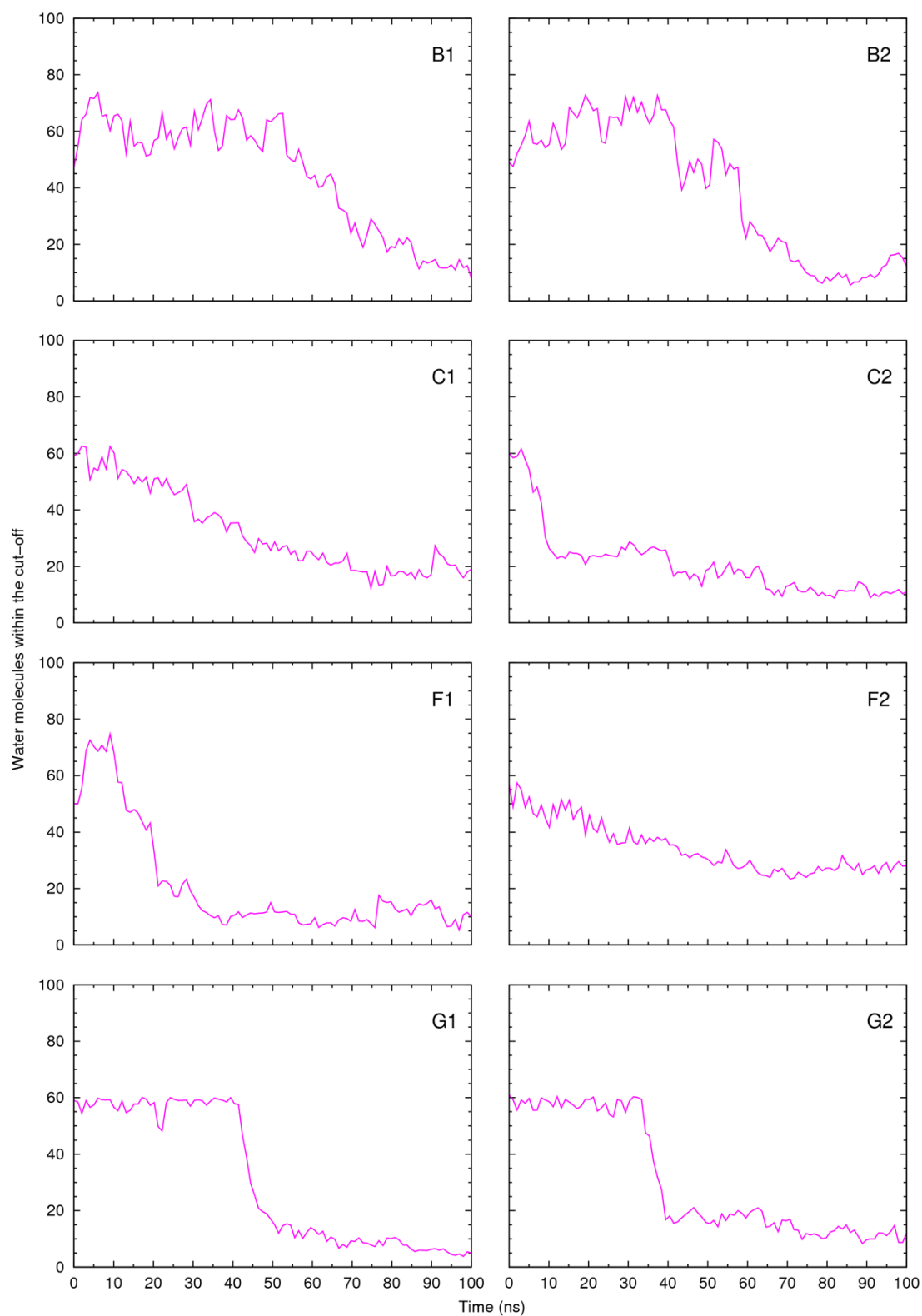


**Figure S9.** Variation in the number of water molecules within the solvation shell defined by a cut-off of 3.5 Å from **1** (simulations B1 and B2), **2** (simulations C1 and C2), **5** (simulations F1 and F2) or **6** (simulations G1 and G2). Data was smoothed using Bézier curves.

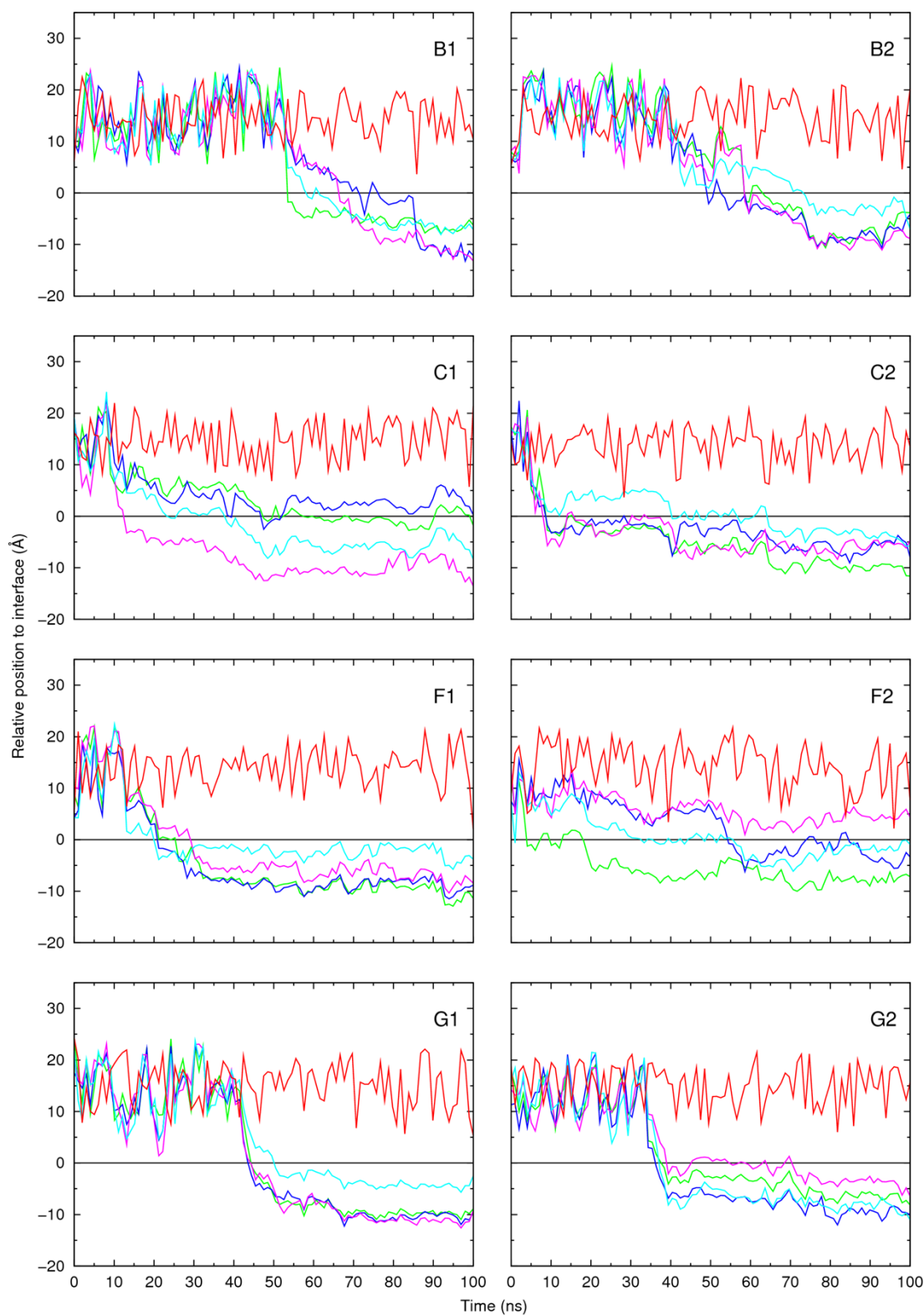


**Figure S10.** Evolution of  $N \cdots P_{int}$  and  $C_n \cdots P_{int}$  distances for **1**, **2**, **5** and **6**, for 100 ns, in simulations B1, B2, C1, C2, F1, F2, G1 and G2.  $C_1$ ,  $C_2$  and  $C_3 \cdots P_{int}$  are shown in green, dark blue and magenta lines,  $N \cdots P_{int}$  is shown as a cyan line, while the water-lipid interface is represented as a black line at  $z = 0$  Å. Data was smoothed using Bézier curves.

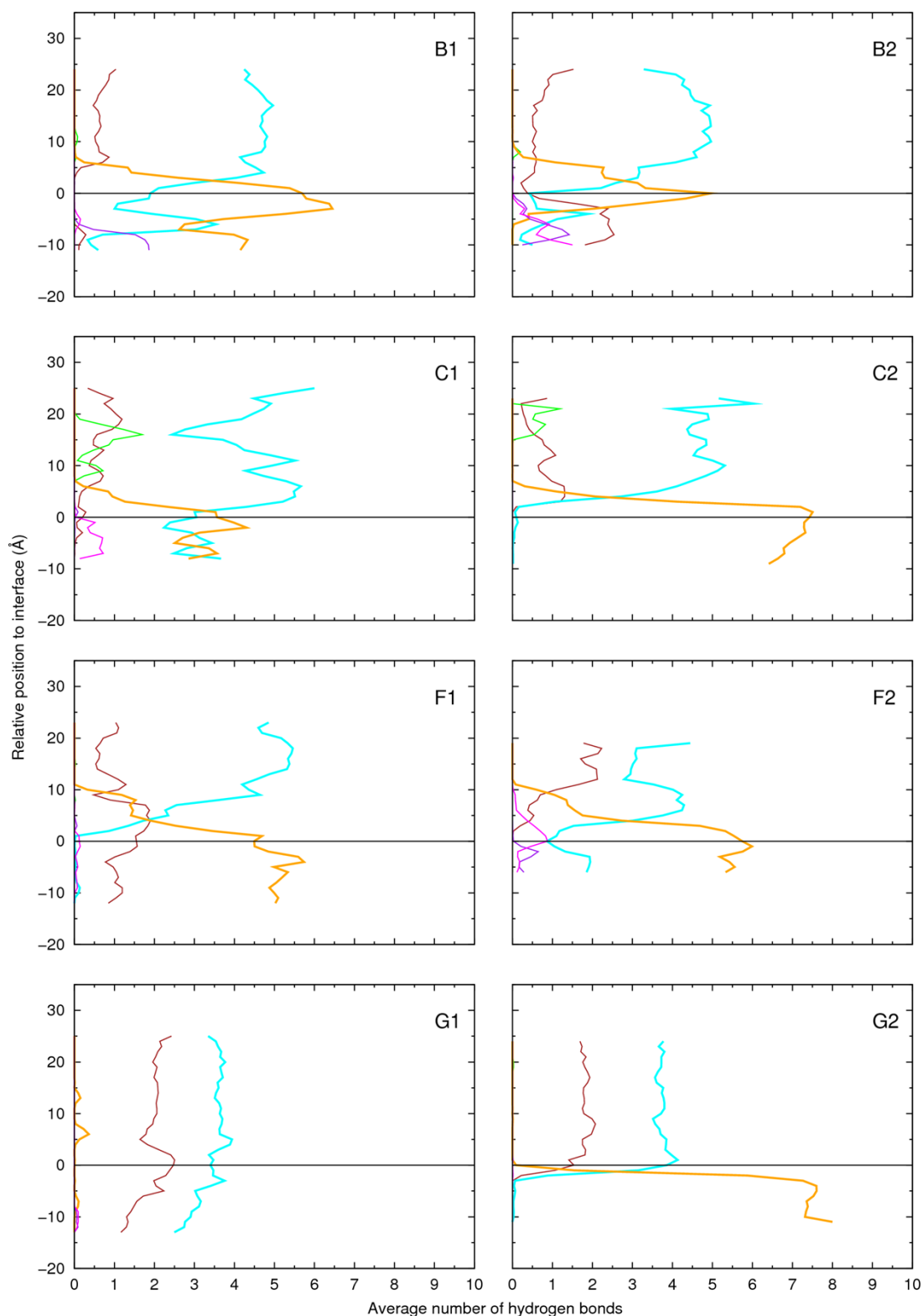


**Figure S11.** Average number of hydrogen bonds vs. the relative position of the COM of **1** (simulations B1 and B2), **2** (simulations C1 and C2), **4** (simulations D1 and D2) and **5** (simulations D1 and D2). The following colour scheme was used for the interactions between the receptor and sulfur atoms (brown), chloride ion (green), water molecules (cyan), POPC head groups (orange), ester groups (purple for the *sn*-1 chains and magenta for the *sn*-2 chains).

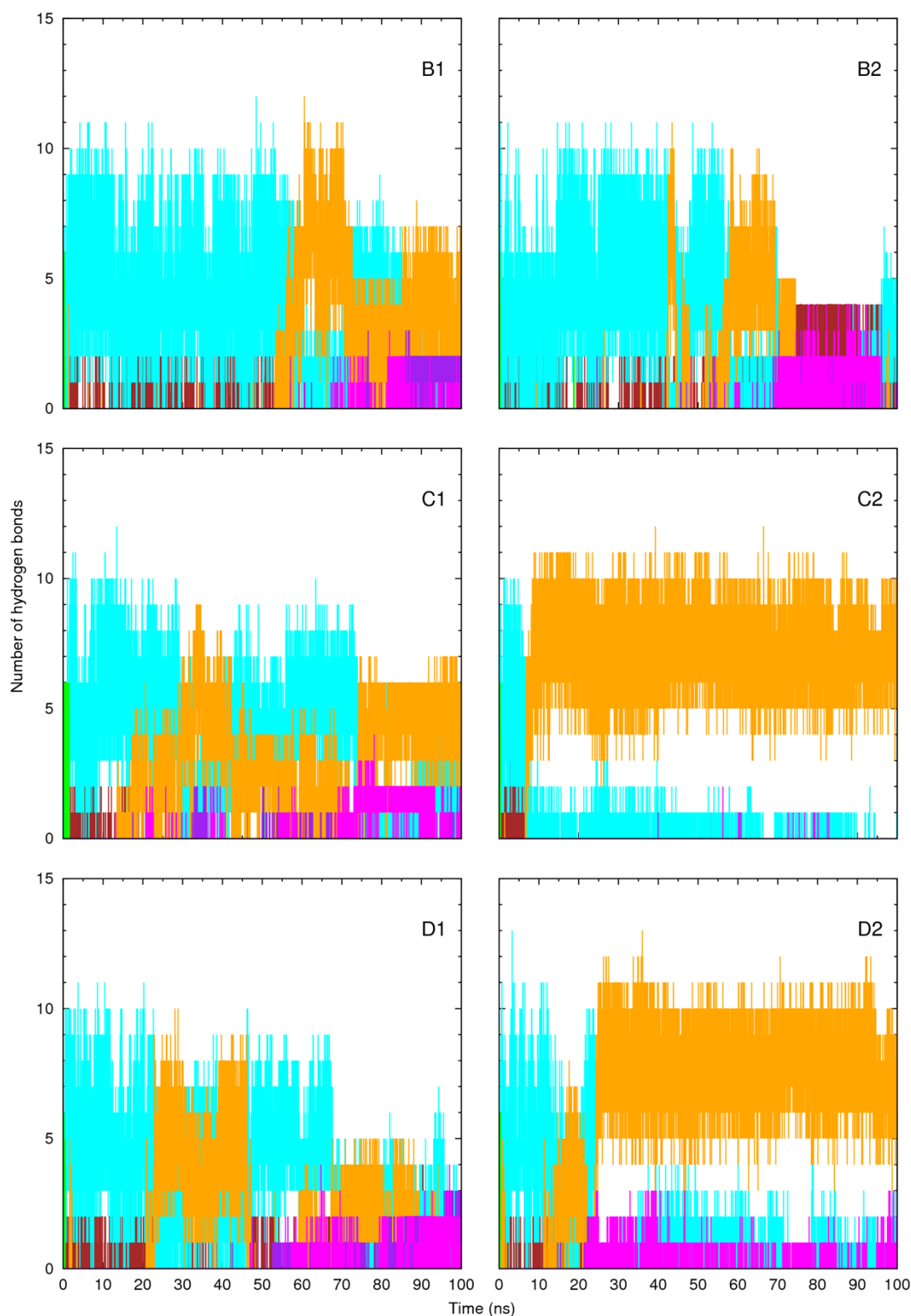


**Figure S12.** Hydrogen bonds counting for the interactions established by the NH groups of **1** (simulations B1 and B2), **2** (simulations C1 and C2) and **3** (simulations D1 and D2). The following colour scheme was used for the interactions: between the receptor and sulfur atoms (brown), chloride ion (green), water molecules (cyan), POPC head groups (orange), ester groups (purple for the *sn*-1 chains and magenta for the *sn*-2 chains).

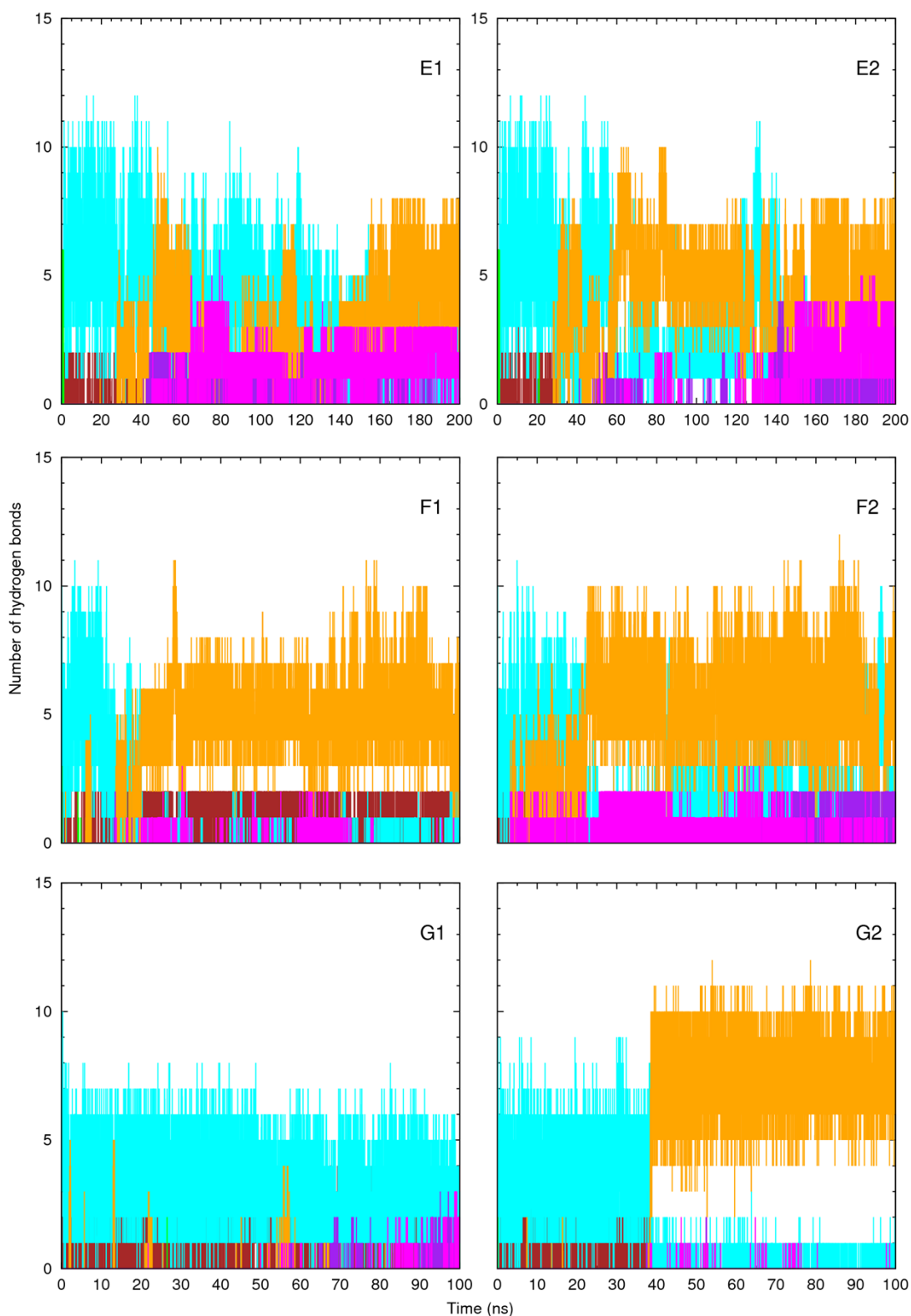


**Figure S13.** Hydrogen bonds counting for the interactions established by the NH groups of **4** (simulations E1 and E2), **5** (simulations F1 and F2) and **6** (simulations G1 and G2). The following colour scheme was used for the interactions: between the receptor and sulfur atoms (brown), chloride ion (green), water molecules (cyan), POPC head groups (orange), ester groups (purple for the *sn*-1 chains and magenta for the *sn*-2 chains).

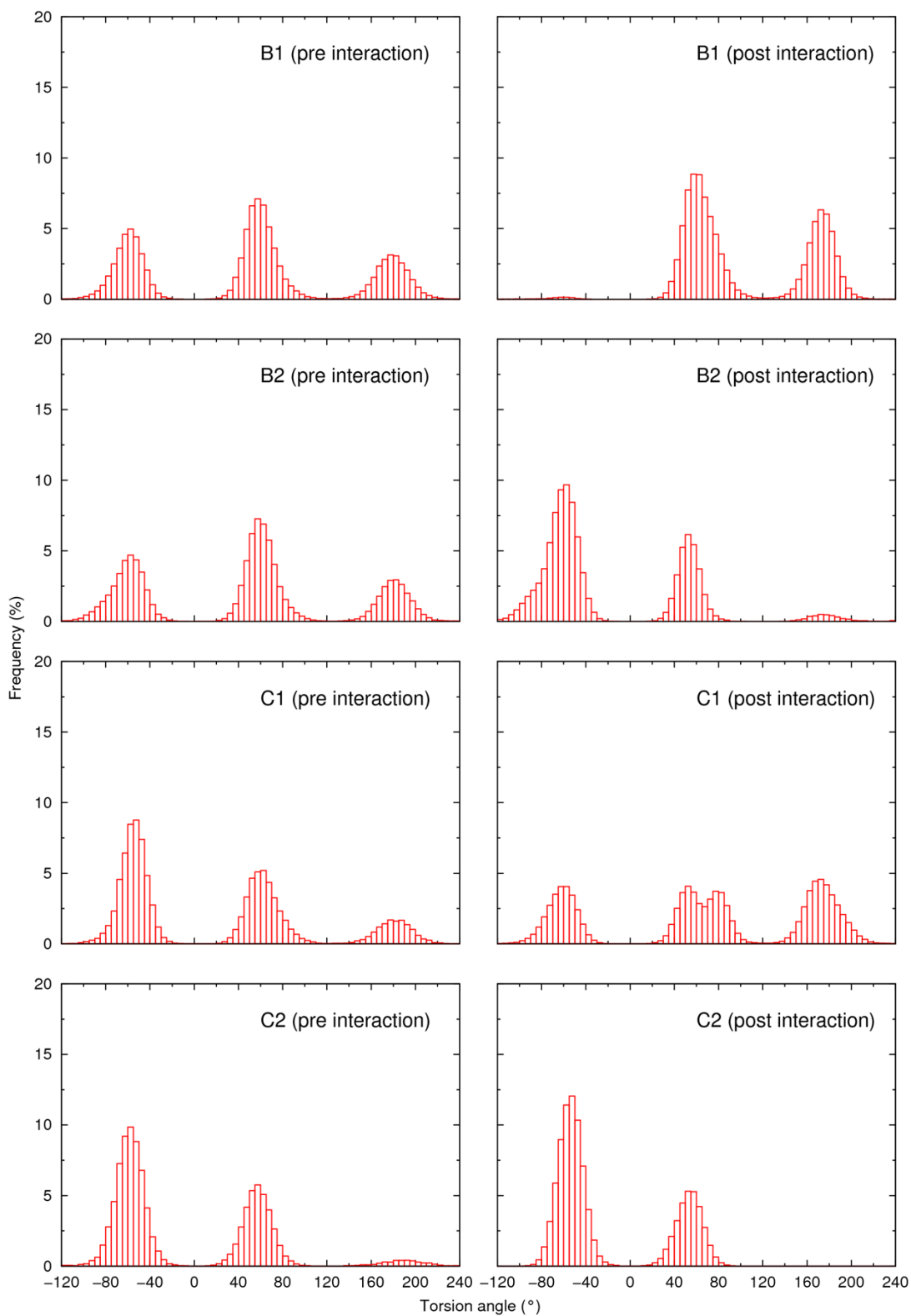


**Figure S14.** Frequency histograms showing the distribution of the three N-C-C-N torsion angles values of **1** and **2** in simulations B1, B2, C1 and C2, before the interaction with the interface (*pre interaction*) and after (*post interaction*).

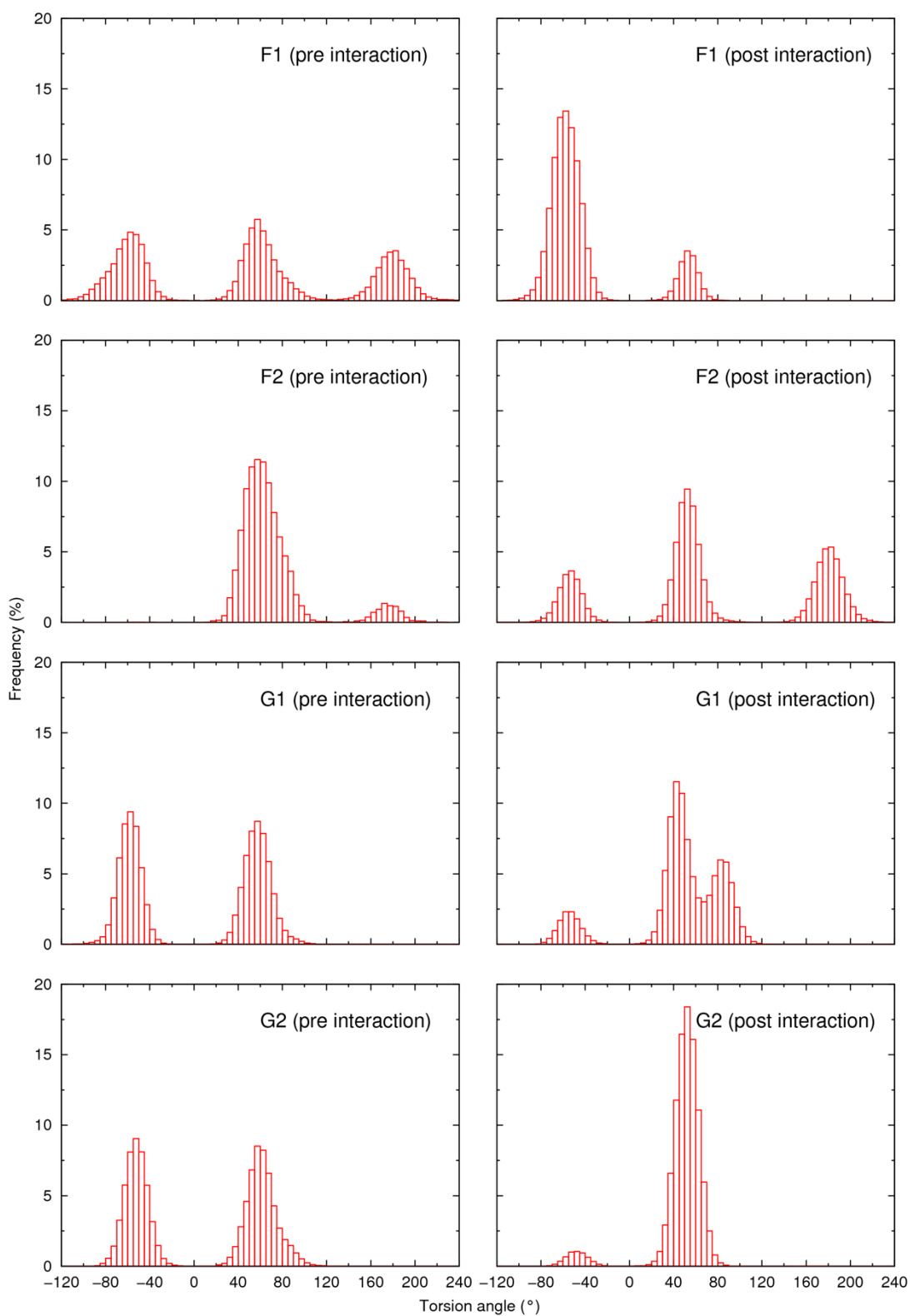


**Figure S15.** Frequency histograms showing the distribution of the three N-C-C-N torsion angles values of **5** and **6** in simulations F1, F2, G1 and G2, before the interaction with the interface (*pre interaction*) and after (*post interaction*).

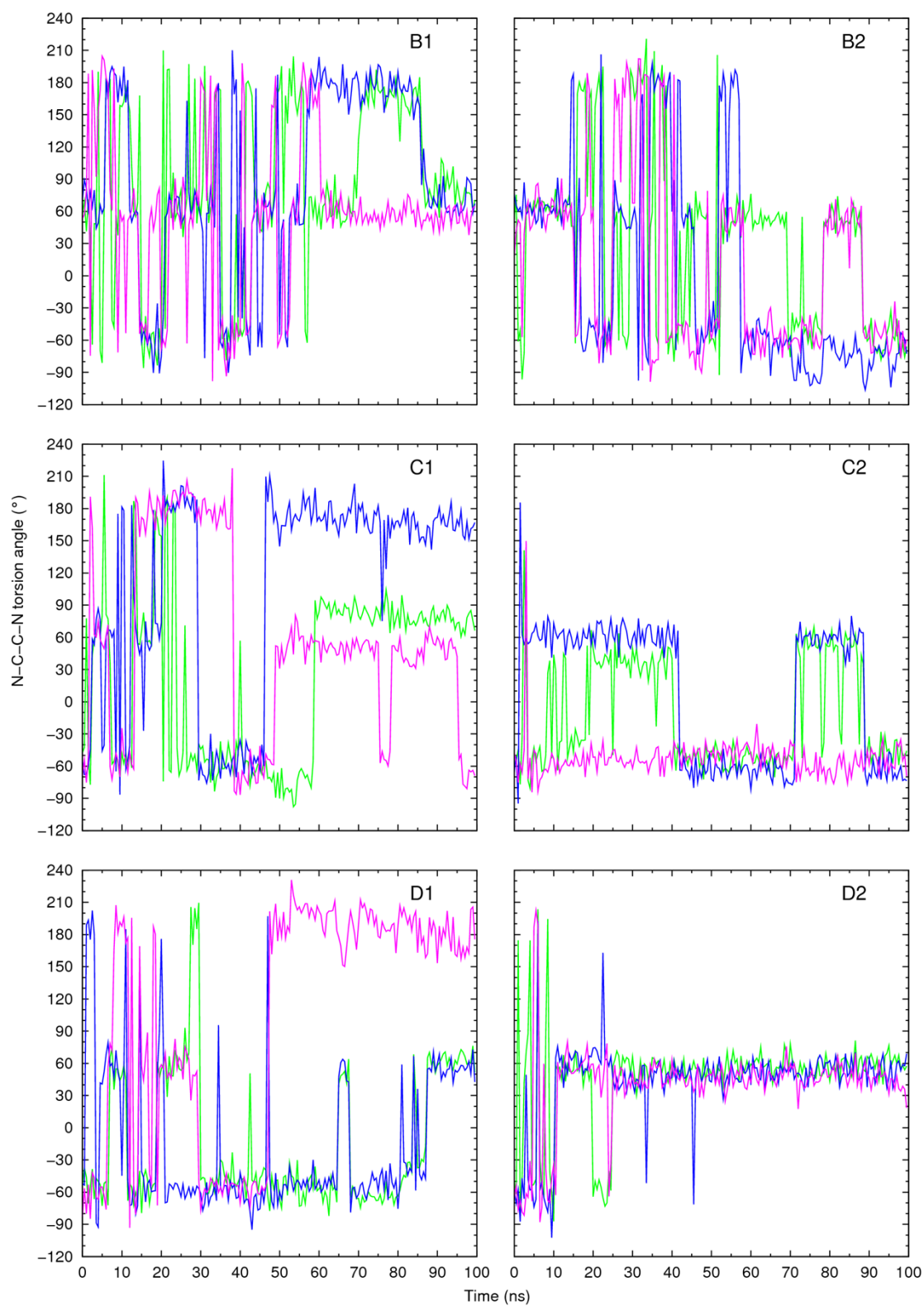


**Figure S16.** Variations in the three N-C-C-N tripodal torsion angles for 100 ns of MD simulation, extracted every 500 ps, for simulations B1, B2, C1, C2, D1 and D2, containing **1**, **2** or **3**.

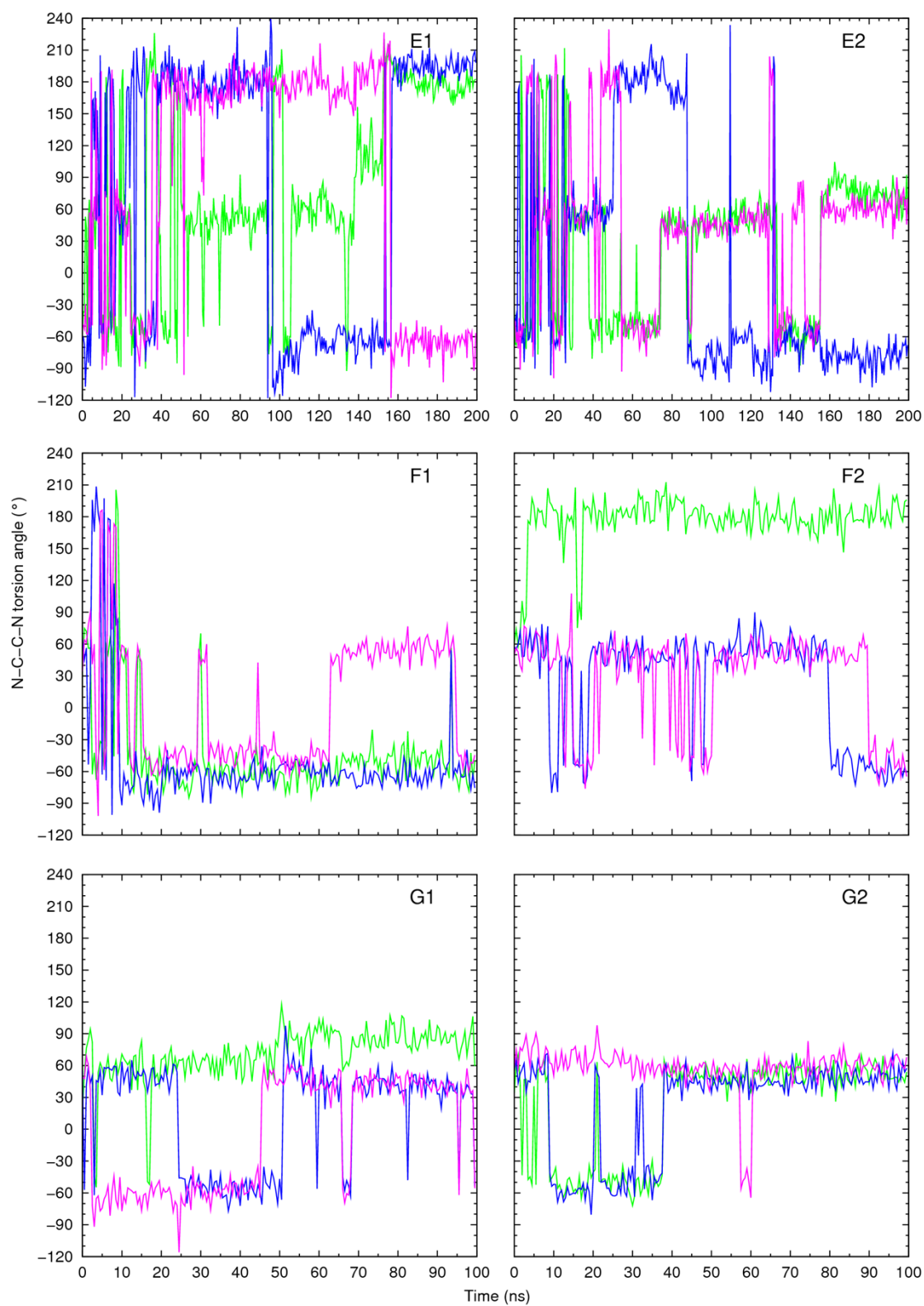


**Figure S17.** Variations in the three N-C-C-N tripodal torsion angles for 200ns of MD simulation E or 100 ns of MD simulations F and G, extracted every 500 ps, for simulations E1, E2, F1, F2, G1 and G2, containing 4, 5 or 6.

## Supporting figures for simulation H

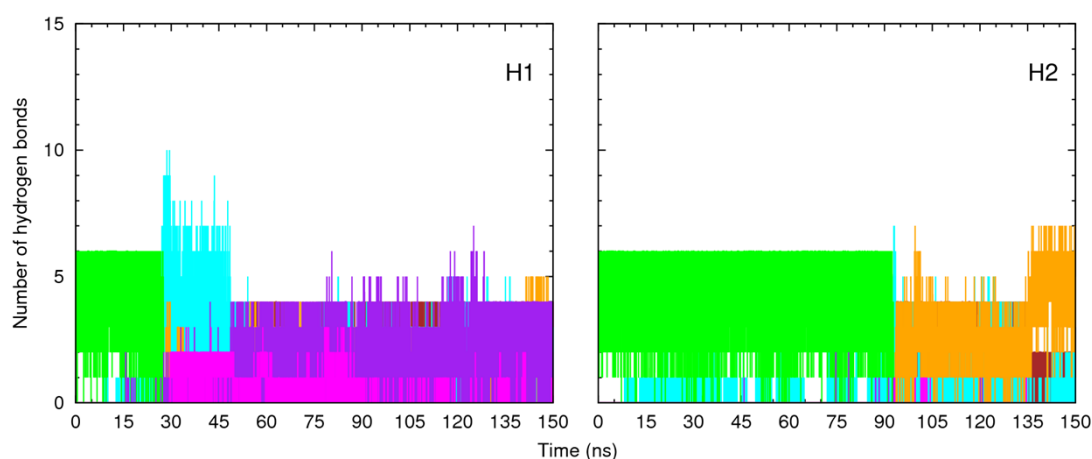


**Figure S18.** Hydrogen bonds counting for the interactions established by the NH groups of **3** (simulations H1 and H2). The following colour scheme was used for the interactions between the receptor and sulfur atoms (brown), chloride ion (green), water molecules (cyan), POPC head groups (orange), ester groups (purple for the *sn*-1 chains and magenta for the *sn*-2 chains).

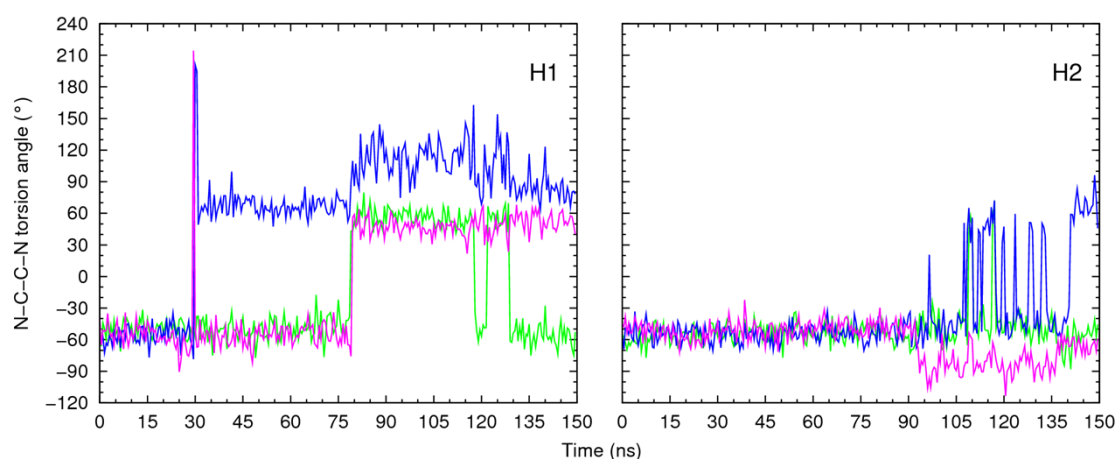


**Figure S19.** Variations in the three N-C-C-N tripodal torsion angles for 150 ns of MD simulation, extracted every 500 ps, for simulations H1 and H2, containing **3**.

## Supporting figures for simulation H'

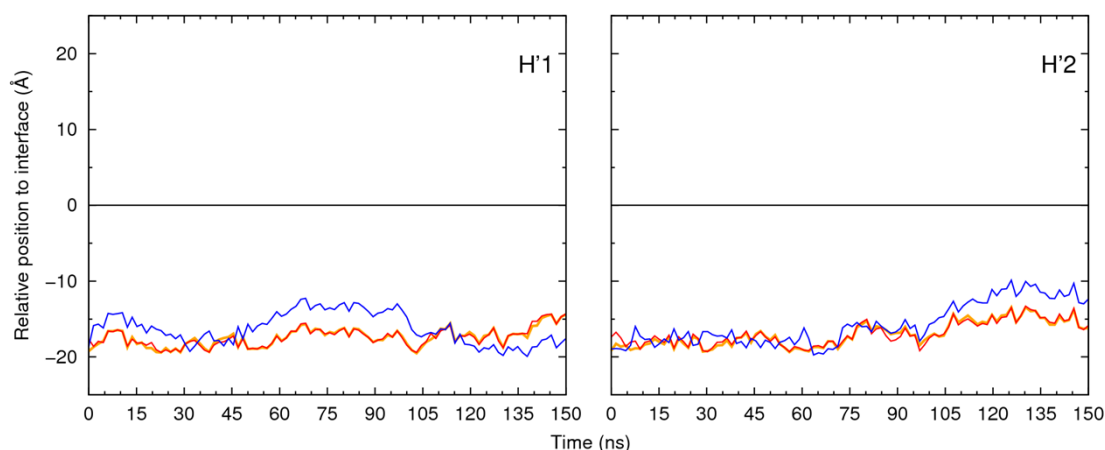


**Figure S20.** Evolution of COM...P<sub>int</sub> distances for **3**, Cl...P<sub>int</sub> and N<sub>C</sub>...P<sub>int</sub> in simulations H'1 and H'2, during the 150 ns of simulation time. COM...P<sub>int</sub> is shown in orange, Cl...P<sub>int</sub> is shown in red, and N<sub>C</sub>...P<sub>int</sub> is shown in blue, while the water-lipid interface is represented as a black line at  $z = 0$  Å.

## Methods of preliminary MD simulation in water solution and supporting figures for simulation E'

Chloride complexes of **1-6** were immersed in cubic boxes containing 3009 TIP3P water molecules, affording systems **a-f** and **g-l**. In the six former systems, the individual N-C-C-N torsion angles of the tripodal molecule were restrained with a 10 kcal/mol rad<sup>2</sup>, while in system **g-l** an additional distance restraint was also applied, as summarized in **Table S10**. The following multi-stage equilibration process was carried out before the 30 ns production.

Initially, the solvent was relaxed by a MM minimization with a harmonic restraint of 500 kcal/mol Å<sup>2</sup> on the anion complexes, followed by a MM minimization of all system. The system was then heated to 303 K during 50 ps using the Langevin thermostat with a collision frequency of 1 ps<sup>-1</sup> in an NVT ensemble, with a 10 kcal/mol Å<sup>2</sup> restraint on the chloride complexes. The density of the system was then adjusted for 1 ns in a NPT ensemble at 1 atm with isotropic pressure scaling using a relaxation time of 1 ps, with the anion complexes still restrained with a 10 kcal/mol Å<sup>2</sup> force constant. The 30 ns collection runs were performed for simulations **a-f** and **g-l**, with the restraints given in **Table S10**.

The SHAKE algorithm<sup>11</sup> was used to constrain all bonds involving hydrogen atoms, allowing the use of a 2 fs time step. An 8 Å cut-off was used for the van der Waals and non-bonded electrostatic interactions. Frames were saved every 1.0 ps leading to trajectory files containing 30000 structures for each simulation. These simulations were performed with *pmemd.cuda* AMBER12 executable, which allowed to accelerate explicit solvent Particle Mesh Ewald (PME)<sup>12</sup> calculations, through the use of GPUs.<sup>13-15</sup>

**Table S10.** Water solution simulated systems at 303 K for 30 ns.

System ID	Transporter	N-C-C-N torsion angle restrains (kcal/mol rad <sup>2</sup> )	Cl <sup>-</sup> ...N distance restrains (kcal/ mol Å <sup>2</sup> )
<b>a</b>	<b>1</b>		
<b>b</b>	<b>2</b>		
<b>c</b>	<b>3</b>		
<b>d</b>	<b>4</b>	10 <sup>a)</sup>	-
<b>e</b>	<b>5</b>		
<b>f</b>	<b>6</b>		
<b>g</b>	<b>1</b>		
<b>h</b>	<b>2</b>		
<b>i</b>	<b>3</b>		
<b>j</b>	<b>4</b>	10 <sup>a)</sup>	1 <sup>b)</sup>
<b>k</b>	<b>5</b>		
<b>l</b>	<b>6</b>		

<sup>a)</sup> This force constant was applied to each one of the three N-C-C-N torsion angles; <sup>b)</sup> This force constant was applied between the anion and the nitrogen atom of an N-H binding unit

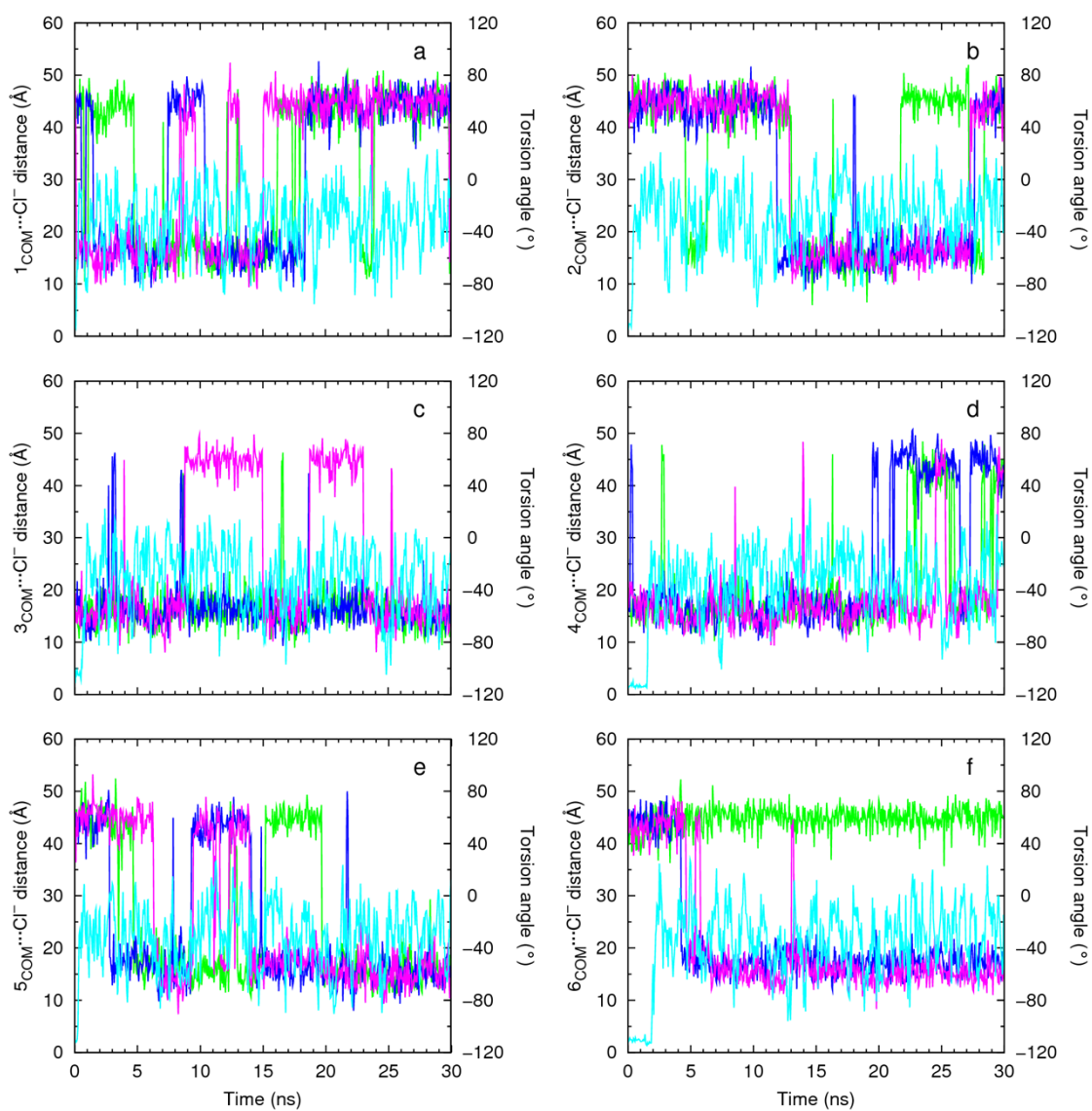


**Figure S21.** Evolution of the  $1-6_{\text{COM}}\cdots\text{Cl}^-$  distances (cyan line) and variations in the three N-C-C-N tripodal torsion angles (blue, green and magenta lines), in simulations **a-f** for 30 ns. All parameters were extracted every 50 ps.

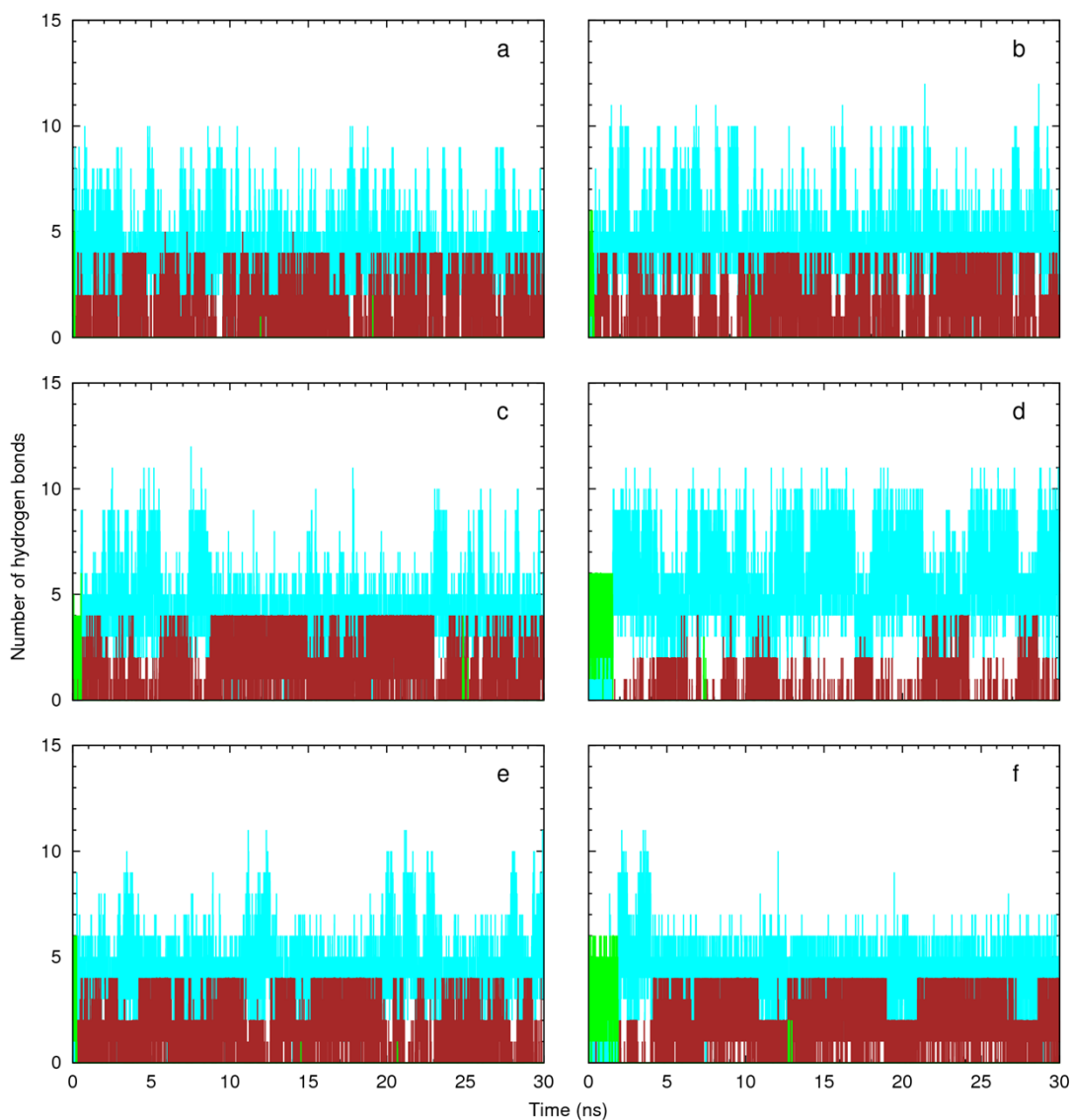


**Figure S22.** Hydrogen bonds counting for the interactions established by the N-H groups of **1-6** in simulations **a-f**. The following colour scheme was used for the interactions between the receptor and sulfur atoms (brown), chloride ion (green), and water molecules (cyan).

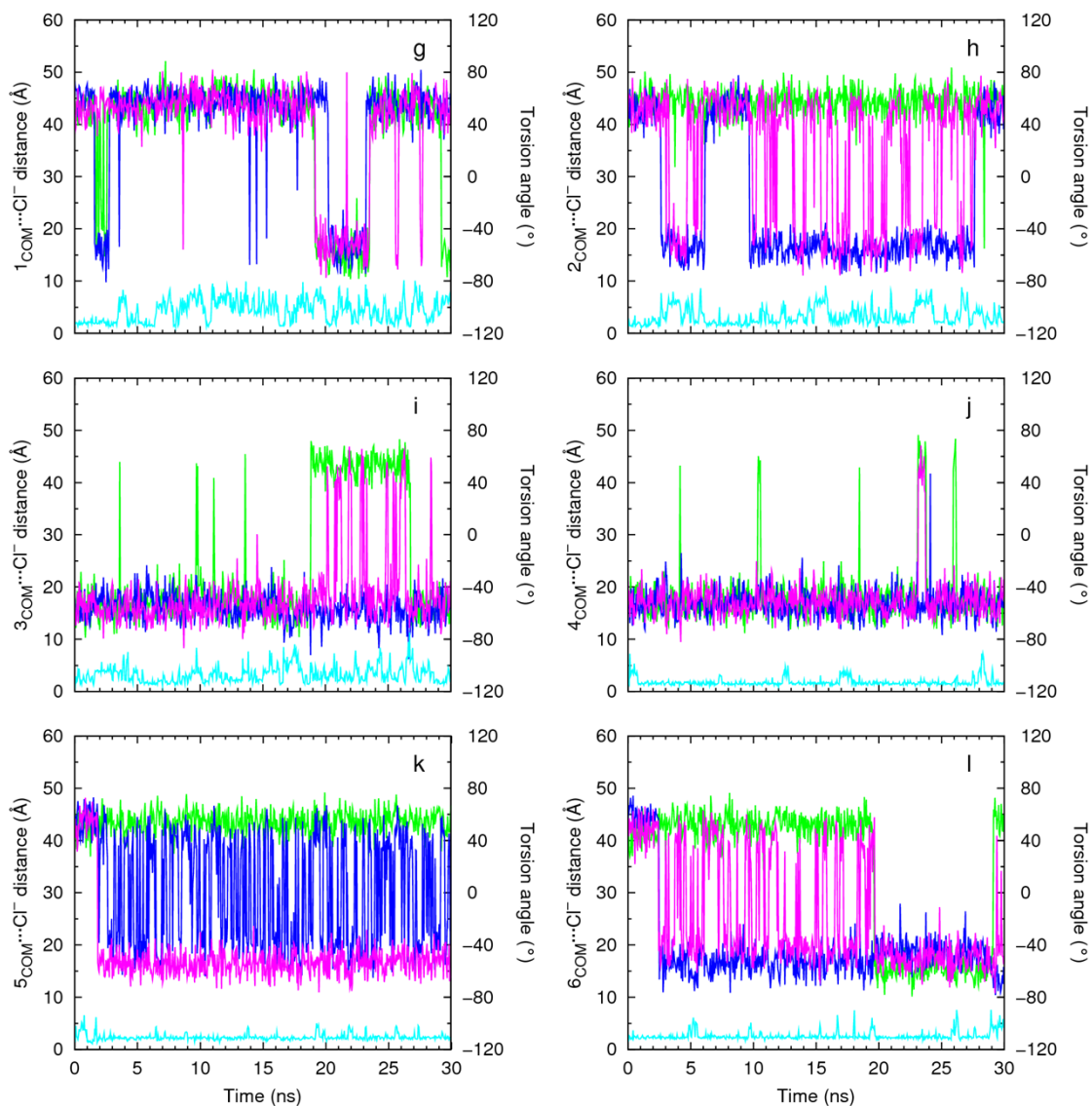


**Figure S23.** Evolution of the  $1-6_{\text{COM}} \cdots \text{Cl}^-$  distances (cyan line) and variations in the three N-C-C-N tripodal torsion angles (blue, green and magenta lines), in simulations **g-l** for 30 ns. All parameters were extracted every 50 ps.

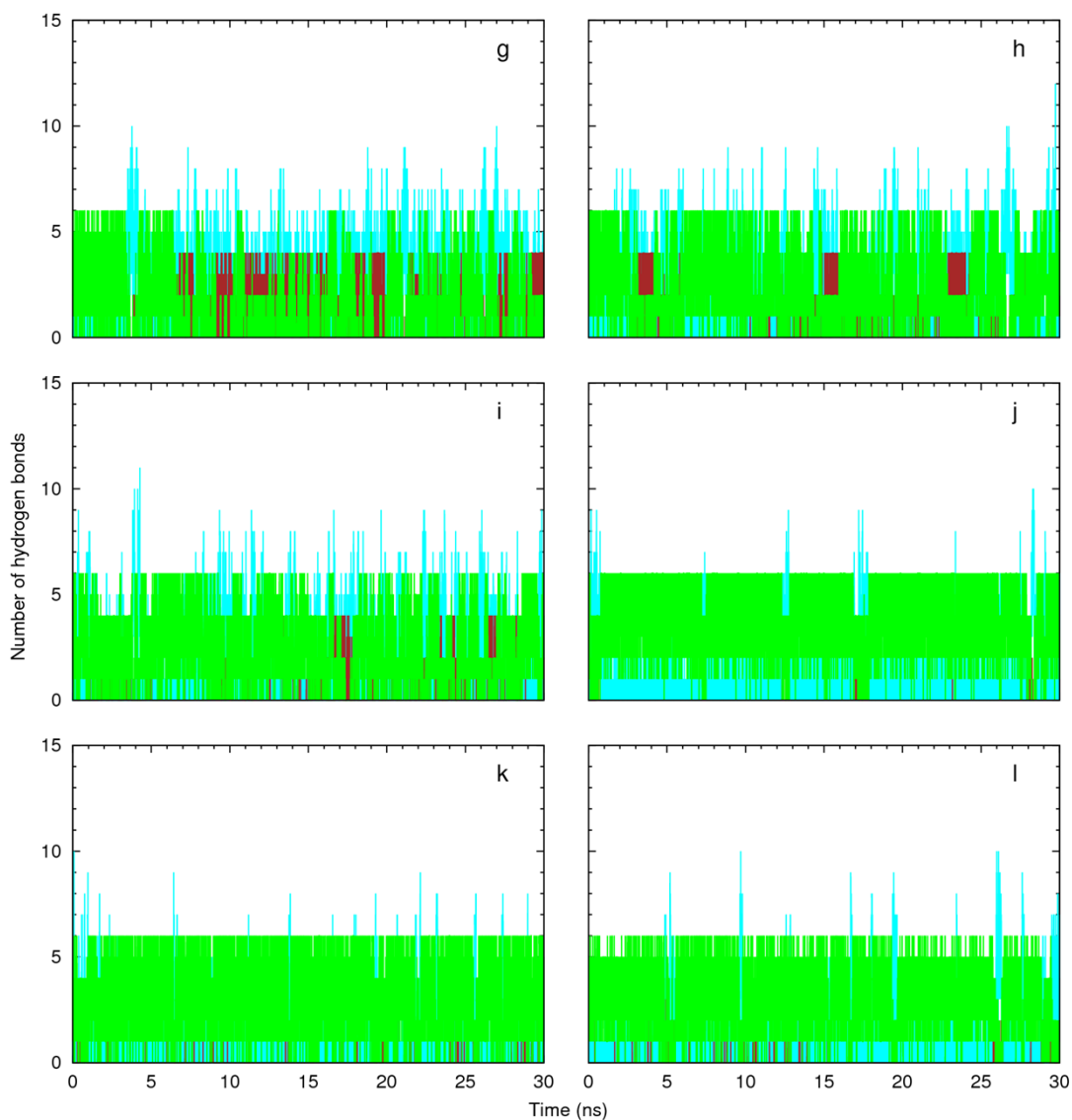


**Figure S24.** Hydrogen bonds counting for the interactions established by the N-H groups of **1-6** in simulations **g-l**. The following colour scheme was used for the interactions between the receptor and sulfur atoms (brown), chloride ion (green), and water molecules (cyan).

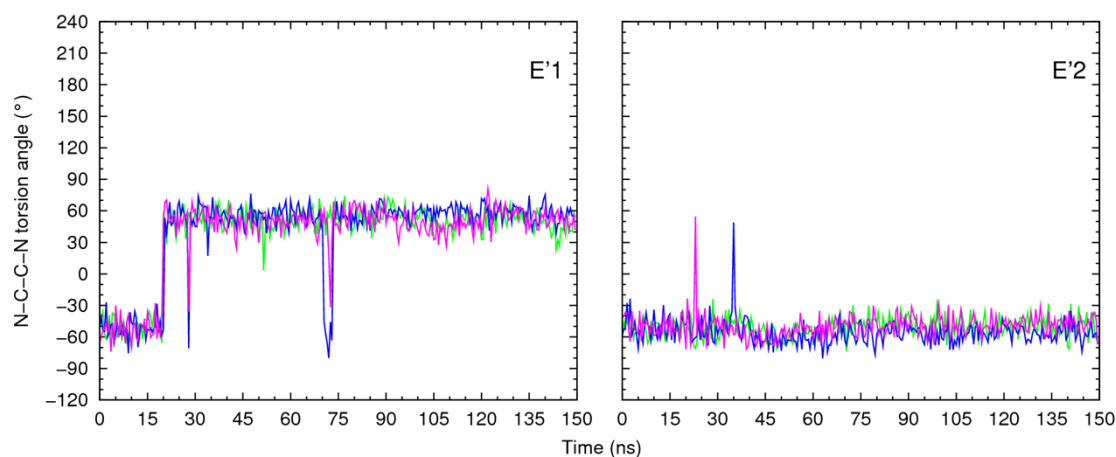


**Figure S25.** Variations in the three N-C-C-N tripodal torsion angles for 150 ns of MD simulations E'1 and E'2, extracted every 500 ps, for simulations E'1 and E22, containing  $4\Rightarrow\text{Cl}^-$ .

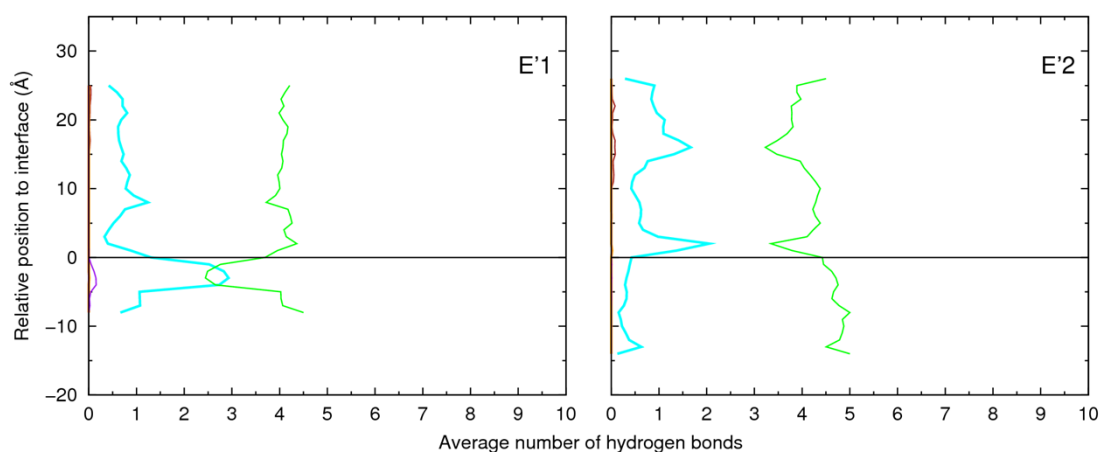


**Figure S26.** Average number of hydrogen bonds vs. the relative position of the COM of **4** (simulations E'1 and E'2). The following colour scheme was used for the interactions between the receptor and sulfur atoms (brown), chloride ion (green), water molecules (cyan), POPC head groups (orange), ester groups (purple for the *sn*-1 chains and magenta for the *sn*-2 chains).

## Supporting figures for the evaluation of the impact of 1-6 onto the POPC membrane

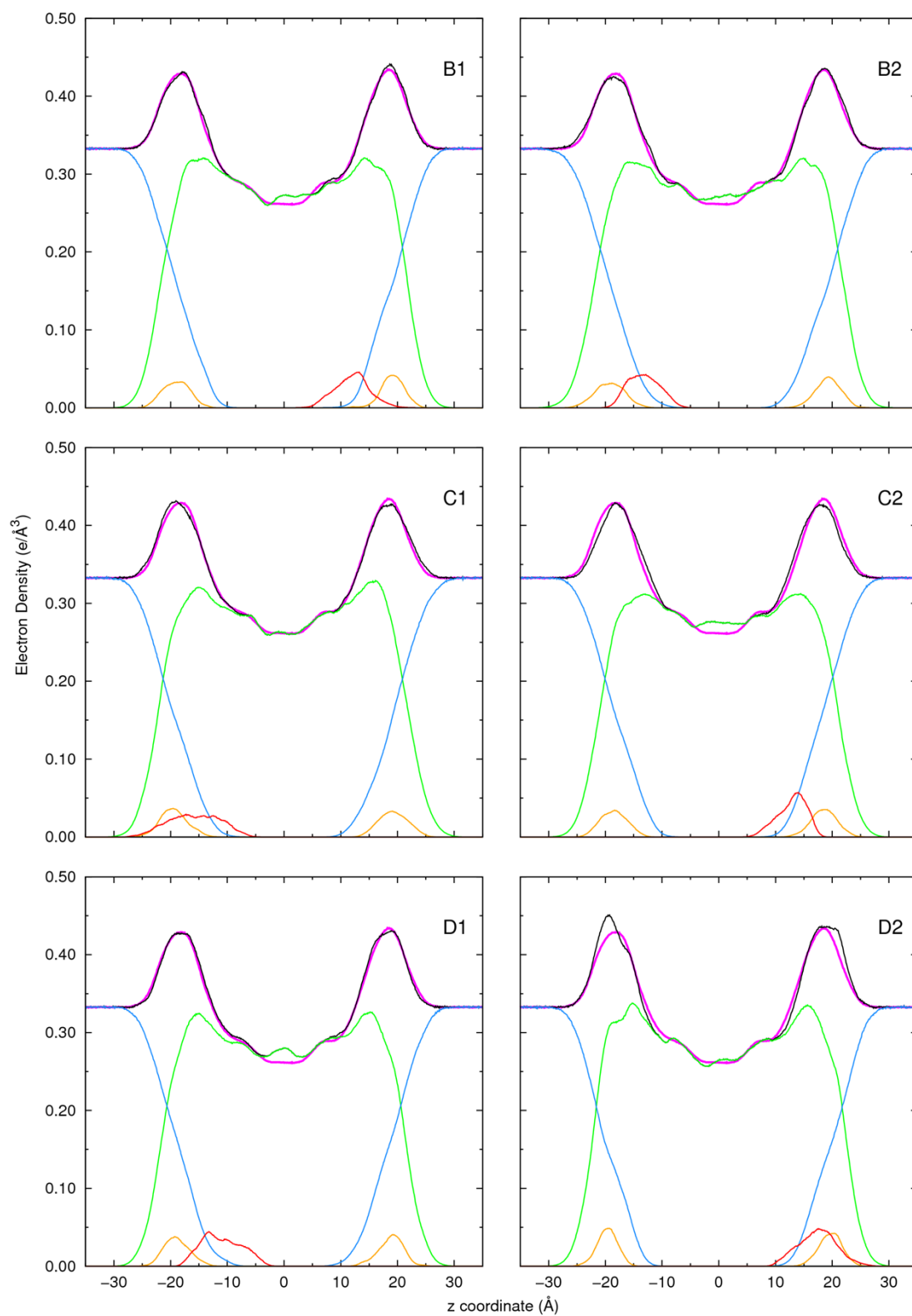


**Figure S27.** Electron density profiles of simulations B1, B2, C1, C2, D1 and D2 with the full system plotted in black, water in blue, phospholipids in green, phosphorus atoms in orange and the corresponding transporter profile in red (scaled 5 times). The  $z = 0 \text{ \AA}$  corresponds to the core of the POPC bilayer. The POPC bilayer profile of system A is also shown as a pink line.

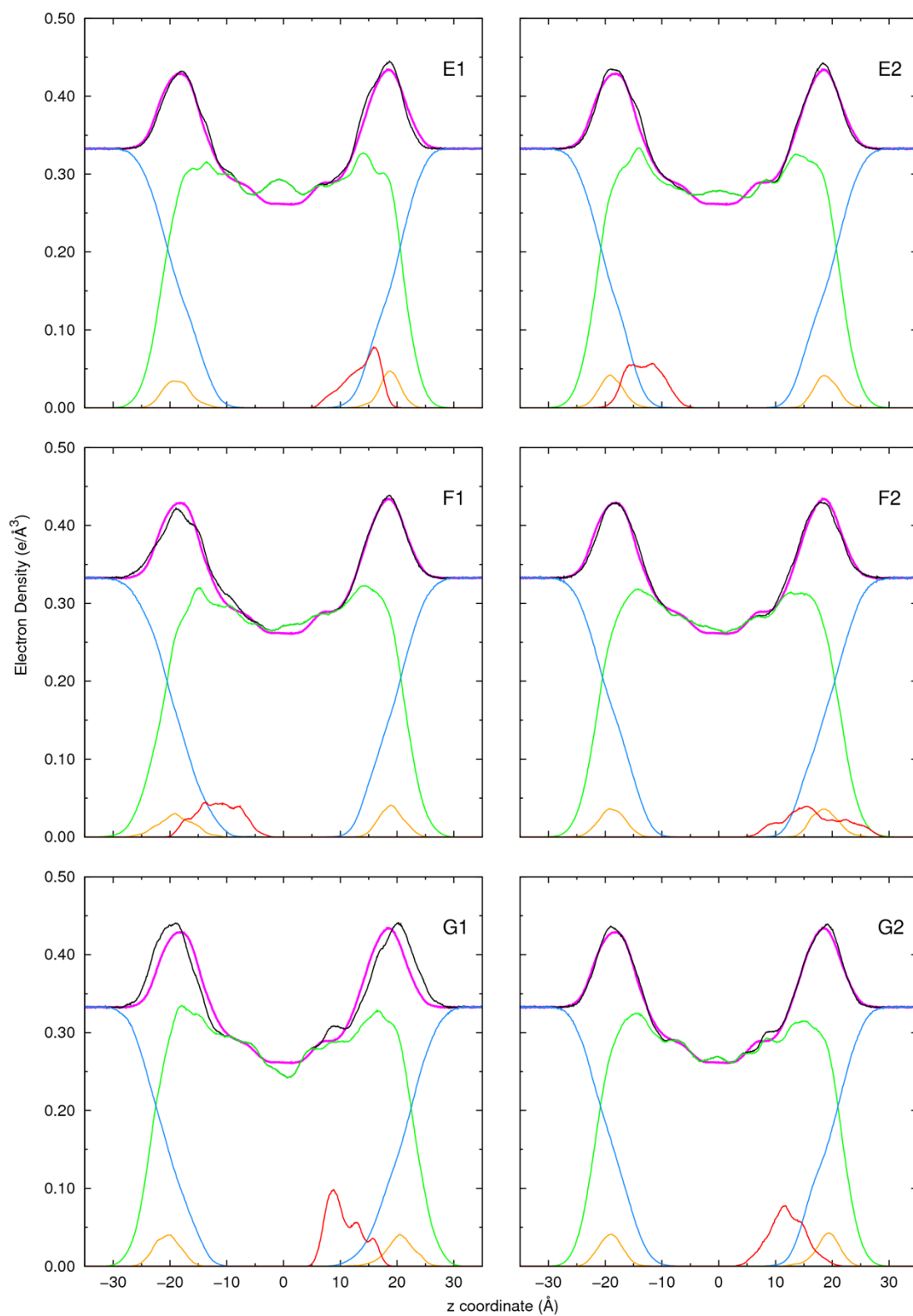


**Figure S28.** Electron density profiles of simulations E1, E2, F1, F2, G1 and G2 with the full system plotted in black, water in blue, phospholipids in green, phosphorus atoms in orange and the corresponding transporter profile in red (scaled 5 times). The  $z = 0 \text{ \AA}$  corresponds to the core of the POPC bilayer. The POPC bilayer profile of system A is also shown as a pink line.

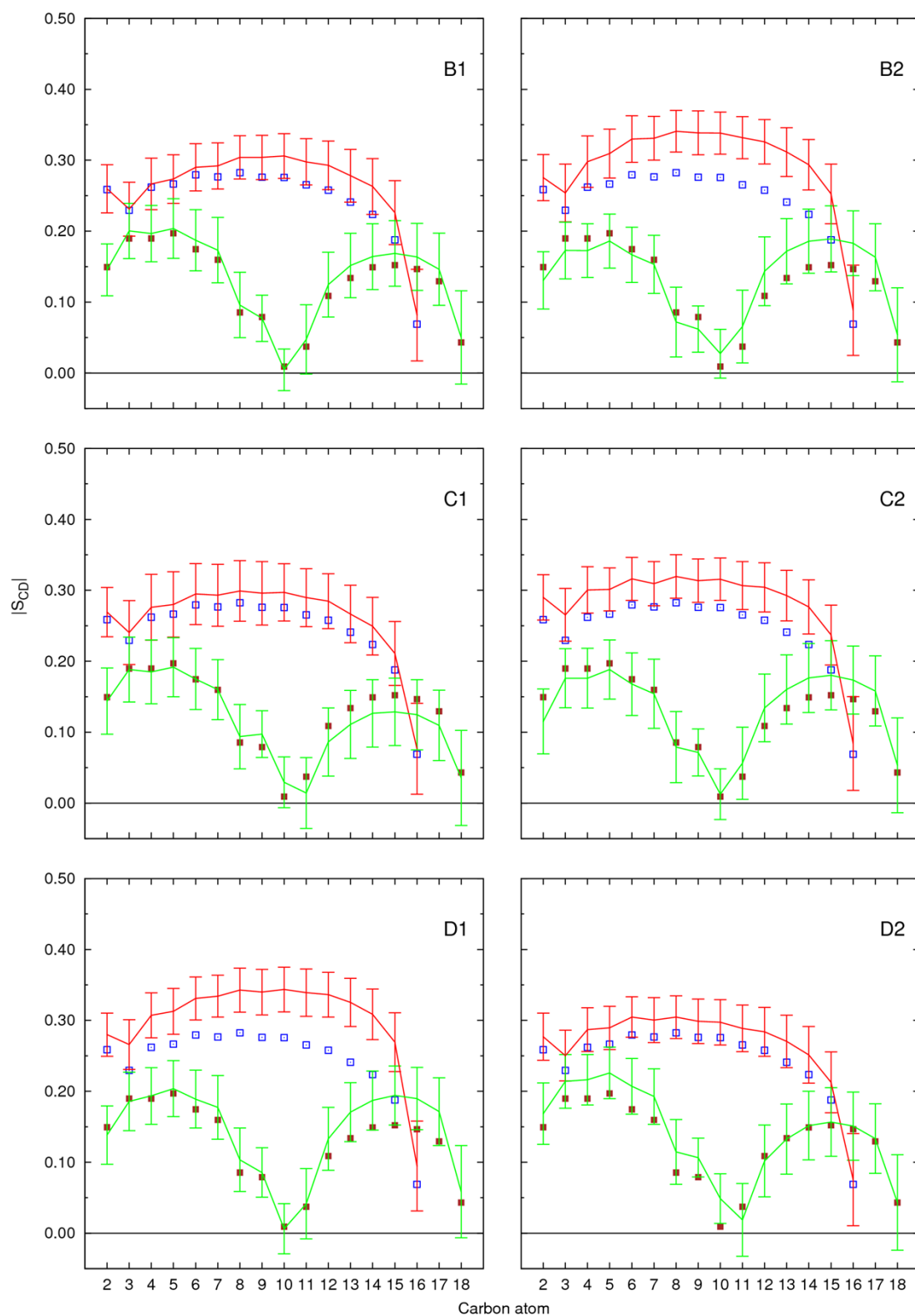


**Figure S29.** Computed  $|S_{CD}|$  for palmitoyl and oleyl chains for 25 ns of sampling of simulations B1, B2, C1, C2, D1 and D2. The  $|S_{CD}|$  values calculated for the  $sn-1$  chain are shown in red, while the values for the  $sn-2$  chain are shown in green. The error bars associated with these results correspond to the SD. The computed  $|S_{CD}|$  values from system A are presented as blue  $\square$  ( $sn-1$  chain), and brown  $\blacksquare$  ( $sn-2$  chain).

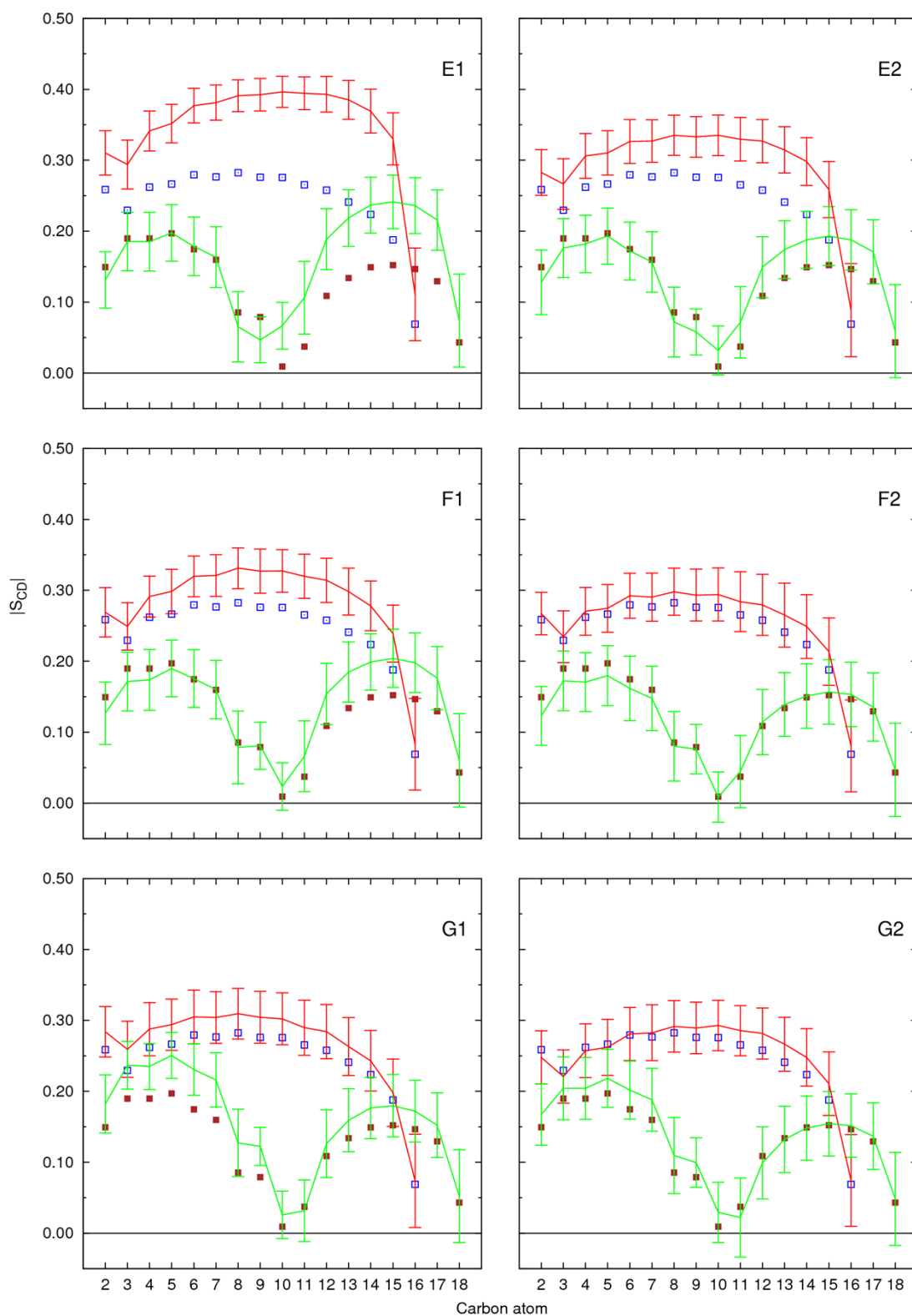


**Figure S30.** Computed  $|S_{CD}|$  for palmitoyl and oleyl chains for 40 ns of sampling of simulations E1, E2, and 25 ns of sampling in simulations F1, F2, G1 and G2. The  $|S_{CD}|$  values calculated for the  $sn-1$  chain are shown in red, while the values for the  $sn-2$  chain are shown in green. The error bars associated with these results correspond to the SD. The computed  $|S_{CD}|$  values from system A are presented as blue  $\square$  ( $sn-1$  chain), and brown  $\blacksquare$  ( $sn-2$  chain).

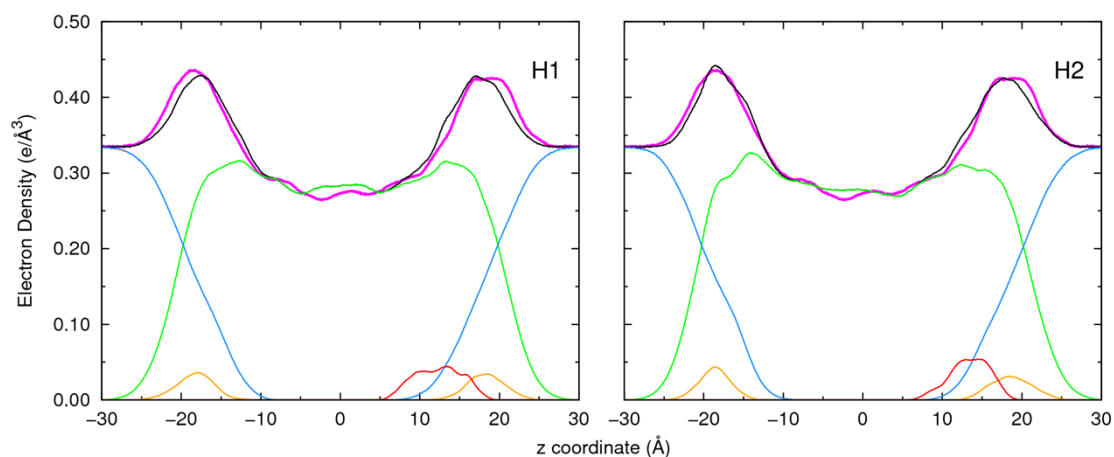


**Figure S31.** Electron density profiles of simulations H1 and H2 with the full system plotted in black, water in blue, phospholipids in green, phosphorus atoms in orange and the 3's profile in red (scaled 5 times). The  $z = 0 \text{ \AA}$  corresponds to the core of the POPC bilayer. The POPC bilayer profile reported on the LIPID11 paper is also shown as a pink line.

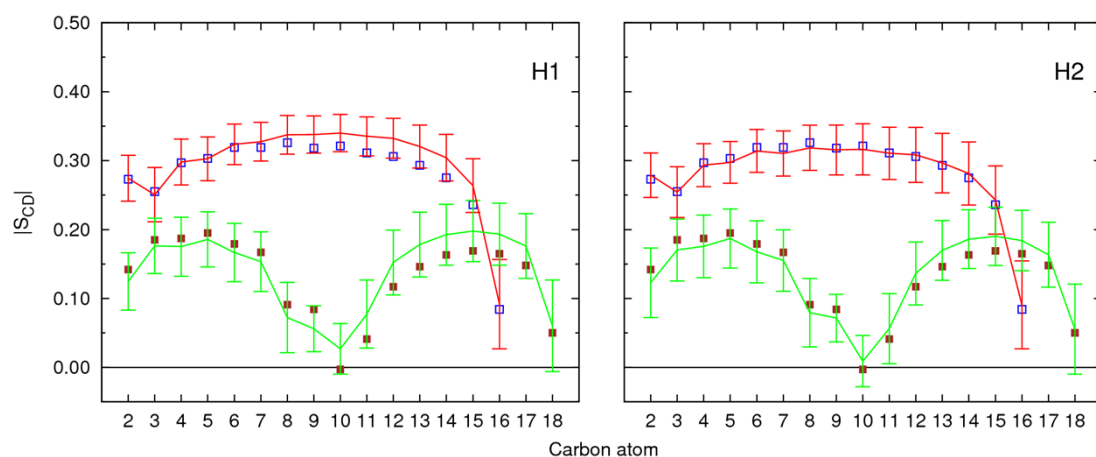


**Figure S32.** Computed  $|S_{CD}|$  for palmitoyl and oleyl chains for 50 ns of sampling of simulations H1 and H2. The  $|S_{CD}|$  values calculated for the *sn*-1 chain are shown in red, while the values for the *sn*-2 chain are shown in green. The error bars associated with these results correspond to the SD. The computed  $|S_{CD}|$  values from the LIPID11 paper are presented as blue  $\square$  (*sn*-1 chain), and brown  $\blacksquare$  (*sn*-2 chain).

## References

1. D. Poger and A. E. Mark, *J. Chem. Theory Comput.*, 2010, **6**, 325-336.
2. N. Kucerka, S. Tristram-Nagle and J. F. Nagle, *J. Membr. Biol.*, 2005, **208**, 193-202.
3. L. Rosso and I. R. Gould, *J. Comput. Chem.*, 2008, **29**, 24-37.
4. S. W. Siu, R. Vacha, P. Jungwirth and R. A. Bockmann, *J. Chem. Phys.*, 2008, **128**, 125103.
5. N. Kucerka, M. P. Nieh and J. Katsaras, *Biochim. Biophys. Acta*, 2011, **1808**, 2761-2771.
6. A. A. Skjevik, B. D. Madej, R. C. Walker and K. Teigen, *J. Phys. Chem. B*, 2012, **116**, 11124-11136.
7. H. Loeffler, Jun 20, 2012 edn., 2010, vol. Jun 20, 2012.
8. T. Huber, K. Rajamoorthi, V. F. Kurze, K. Beyer and M. F. Brown, *J. Am. Chem. Soc.*, 2002, **124**, 298-309.
9. J. Seelig and N. Waespe-Sarcevic, *Biochemistry*, 1978, **17**, 3310-3315.
10. B. Perly, I. C. P. Smith and H. C. Jarrell, *Biochemistry*, 1985, **24**, 1055-1063.
11. J.-P. Ryckaert, G. Ciccotti and H. J. C. Berendsen, *J. Comput. Phys.*, 1977, **23**, 327-341.
12. T. Darden, D. York and L. Pedersen, *J. Chem. Phys.*, 1993, **98**, 10089-10092.
13. A. W. Gotz, M. J. Williamson, D. Xu, D. Poole, S. Le Grand and R. C. Walker, *J. Chem. Theory Comput.*, 2012, **8**, 1542-1555.
14. R. Salomon-Ferrer, A. W. Götz, D. Poole, S. Le Grand and R. C. Walker, *J. Chem. Theory Comput.*, 2013, 130820111500003.
15. S. Le Grand, A. W. Götz and R. C. Walker, *Comput. Phys. Commun.*, 2013, **184**, 374-380.